Acknowledgments—We thank Dr. K. Yamamoto (The Chemo-Sero-Therapeutic Research Institute) for providing NDV stocks. We also thank the Division of Functional Genomics, Center for Frontier Life Sciences, Nagasaki University, for the autosequencing. We thank Dr. C. Kojima (Graduate School of Biological Science, Nara Institute of Science and Technology) and Dr. T. Fujita (The Tokyo Metropolitan Institute of Medical Science) for helpful discussions and comments on our manuscript.

REFERENCES

1. Sen, G. C., and Lengyel, P. (1992) *J. Biol. Chem.* 267, 5017–5020
2. Samuel, C. (2001) *Clin. Microbiol. Rev.* 14, 778–809
3. Sato, M., Suemori, H., Hata, N., Asagiri, M., Ogasawara, K., Nakao, K., Nakaya, T., Katsuki, M., Noguchi, S., Tanaka, N., and Taniguchi, T. (2000) *Immunity* 13, 539–548
4. Nakaya, T., Sato, M., Hata, N., Asagiri, M., Suemori, H., Noguchi, S., Tanaka, N., and Taniguchi, T. (2001) *Biochem. Biophys. Res. Commun.* 283, 1150–1156
5. Lin, R., Genin, P., Mamane, Y., and Hiscott, J. (2000) *Mol. Cell. Biol.* 20, 6342–6353
6. Lin, R., Mamane, Y., and Hiscott, J. (1999) *Mol. Cell. Biol.* 19, 2465–2474
7. Suhara, W., Yoneyama, M., Iwamura, T., Yoshimura, S., Tamura, K., Namiki, H., Aimoto, S., and Fujita, T. (2000) *J. Biochem. (Tokyo)* 128, 301–307
8. Suhara, W., Yoneyama, M., Kitabayashi, I., and Fujita, T. (2002) *J. Biol. Chem.* 277, 22304–22313
9. Yoneyama, M., Suhara, W., Fukuhara, Y., Fukuda, M., Nishida, E., and Fujita, T. (1998) *EMBO J.* 17, 1087–1095
10. Fitzgerald, K. A., McWhirter, S. M., Faia, K. L., Rowe, D. C., Latz, E., Golenbock, D. T., Coyle, A. J., Liao, S. M., and Maniatis, T. (2003) *Nat. Immunol.* 4, 491–496
11. Sharma, S., tenOever, B. R., Grandvaux, N., Zhou, G. P., Lin, R., and Hiscott, J. (2003) *Science* 300, 1148–1151
12. Vilcek, J., and Sen., G. (1996) *Virology* 375–399
13. Takahasi, K., Suzuki, N. N., Horiuchi, M., Mori, M., Suhara, W., Okabe, Y., Fukuhara, Y., Terasawa, H., Akira, S., Fujita, T., and Inagaki, F. (2003) *Nat. Struct. Biol.* 10, 922–927
14. Qin, B. Y., Liu, C., Lam, S. S., Srinath, H., Delston, R., Correia, J. J., Derynck, R., and Lin, K. (2003) *Nat. Struct. Biol.* 10, 913–921
15. Price, E. R., Jin, M., Lim, D., Pati, S., Walsh, C. T., and McKeon, F. D. (1994) *Proc. Natl. Acad. Sci. U. S. A.* 91, 3931–3935
16. Dove, S., Joung, J., and Hochschild, A. (1997) *Nature* 386, 627–630
17. Hu, J. C., Kornacker, M. G., and Hochschild, A. (2000) *Methods* 20, 80–94
18. Nagata, T., Kishi, H., Liu, Q. L., Yoshino, T., Matsuda, T., Jin, Z. X., Murayama, K., Tsukada, K., and Muraguchi, A. (2000) *J. Immunol.* 165, 4281–4289
19. Montague, J. W., Hughes, F. M., Jr., and Cidlowski, J. A. (1997) *J. Biol. Chem.* 272, 6677–6684
20. Lin, R., Heylbroeck, C., Pitha, P. M., and Hiscott, J. (1998) *Mol. Cell. Biol.* 18, 2986–2996
21. Servant, M. J., Grandvaux, N., tenOever, B. R., Duguay, D., Lin, R., and Hiscott, J. (2003) *J. Biol. Chem.* 278, 9441–9447
22. Iwamura, T., Yoneyama, M., Yamaguchi, K., Suhara, W., Mori, W., Shiota, K., Okabe, Y., Namiki, H., and Fujita, T. (2001) *Genes Cells* 6, 375–388
23. Mori, M., Yoneyama, M., Ito, T., Takahashi, K., Inagaki, F., and Fujita, T. (2004) *J. Biol. Chem.* 279, 9698–9702
24. Kay, J. E. (1996) *Biochem. J.* 314, 361–385
25. Lopez-Ilasaca, M., Schiene, C., Kullertz, G., Tradler, T., Fischer, G., and Wetzker, R. (1998) *J. Biol. Chem.* 273, 9430–9434
26. Leverson, J. D., and Ness, S. A. (1998) *Mol. Cell* 1, 203–211
27. Rycyzyn, M. A., Reilly, S. C., O'Malley, K., and Clevenger, C. V. (2000) *Mol. Endocrinol.* 14, 1175–1186
28. Rycyzyn, M. A., and Clevenger, C. V. (2002) *Proc. Natl. Acad. Sci. U. S. A.* 99, 6790–6795
29. Mamane, Y., Sharma, S., Petropoulos, L., Lin, R., and Hiscott, J. (2000) *Immunity* 12, 129–140

Journal of General Virology (2005), 86, 645–656 DOI 10.1099/vir.0.80479-0

Genetic variation and dynamics of hepatitis C virus replicons in long-term cell culture

Nobuyuki Kato,[1] Takashi Nakamura,[1] Hiromichi Dansako,[1] Katsuyuki Namba,[2] Ken-ichi Abe,[1] Akito Nozaki,[1] Kazuhito Naka,[1] Masanori Ikeda[1] and Kunitada Shimotohno[3]

[1,2]Department of Molecular Biology[1] and First Department of Internal Medicine[2], Okayama University Graduate School of Medicine and Dentistry, 2-5-1 Shikata-cho, Okayama 700-8558, Japan

[3]Department of Viral Oncology, Institute for Virus Research, Kyoto University, 53 Kawara-cho Shogo-in, Sakyo-ku, Kyoto 606-8507, Japan

Correspondence
Nobuyuki Kato
nkato@md.okayama-u.ac.jp

Received 29 July 2004
Accepted 30 November 2004

Hepatitis C virus (HCV) genomic sequences are known to vary widely among HCV strains, but to date there have been few reports on the genetic variations and dynamics of HCV in an experimental system of HCV replication. In this study, a genetic analysis of HCV replicons obtained in long-term culture of two HCV replicon cells (50-1 and 1B-2R1), which were established from two HCV strains, 1B-1 and 1B-2, respectively, was performed. One person cultured 50-1 cells for 18 months, and two people independently cultured 50-1 cells for 12 months. 1B-2R1 cells were also cultured for 12 months. The whole nucleotide sequences of the three independent replicon RNA clones obtained at several time points were determined. It was observed that genetic mutations in both replicons accumulated in a time-dependent manner, and that the mutation rates of both replicons were approximately $3{\cdot}0 \times 10^{-3}$ base substitutions/site/year. The genetic diversity of both replicons was also enlarged in a time-dependent manner. The colony formation assay by transfection of total RNAs isolated from both replicon cells at different time points into naïve HuH-7 cells revealed that the genetic mutations accumulating with time in both replicons apparently improved colony formation efficiency. Taken together, these results suggest that the HCV replicon system is useful for the analysis of evolutionary dynamics and variations of HCV. Using this replicon cell culture system, it was demonstrated further that neither ribavirin nor its derivative mizoribine accelerated the mutation rate or the increase in the genetic diversity of HCV replicon.

INTRODUCTION

Hepatitis C virus (HCV) infection frequently causes chronic hepatitis (Choo *et al.*, 1989; Kuo *et al.*, 1989), which progresses to liver cirrhosis and hepatocellular carcinoma (Ohkoshi *et al.*, 1990; Saito *et al.*, 1990). HCV belongs to the family *Flaviviridae*, whose genome consists of a positive-stranded RNA molecule of 9·6 kb and encodes a large polyprotein precursor of about 3000 aa residues (Kato *et al.*, 1990a; Tanaka *et al.*, 1995). This polyprotein is processed by a combination of the host and viral proteases into at least 10 proteins: the core, envelope 1 (E1), E2, p7, and non-structural protein 2 (NS2), NS3, NS4A, NS4B, NS5A and NS5B (Grakoui *et al.*, 1993; Hijikata *et al.*, 1991, 1993; Mizushima *et al.*, 1994). These HCV proteins not only function in virus replication but may also affect a variety of cellular functions, including gene expression, signal transduction and apoptosis (Bartenschlager & Lohmann, 2000; Kato, 2001).

The most characteristic feature of the HCV genome is its remarkable genetic diversity and variation. To date, more than 50 HCV genotypes have been identified worldwide (Bukh *et al.*, 1995; Simmonds, 1995; Tokita *et al.*, 1996). Each of these genotypes shows more than 20 % difference at the nucleotide level and more than 15 % difference at the amino acid level compared with any of the other genotypes, although the 5′ untranslated regions (5′ UTRs) and core protein-encoding regions are highly homologous among the 50 genotypes (homology of > 90 %). Comparisons of HCV genomes that belong to a single genotype have revealed 5–8 % diversity in nucleotide sequences and 4–5 % diversity in amino acid sequences (Kato *et al.*, 1990b; Kato, 2001). An analysis of the genetic diversity among the HCV genomes in an individual revealed that the diversity in nucleotide sequences averaged 0·9 %, and distributed throughout

Supplementary material is available in JGV Online.

the genome except in the 5′ UTR (Tanaka *et al.*, 1992). This so-called 'quasispecies' nature of the HCV genome has generally been observed in a single patient with chronic hepatitis C (Kato *et al.*, 1992; Martell *et al.*, 1992). This remarkable genetic diversity of the HCV genome suggests that HCV frequently causes mutations of the viral genome.

To date, two groups have estimated the mutation rate of the HCV genome using specimens from a chimpanzee (interval of 8 years) and a patient (interval of 13 years) infected with HCV (Ogata *et al.*, 1991; Okamoto *et al.*, 1992). They estimated that the mutation rate of the HCV genome was $1{\cdot}4–1{\cdot}9 \times 10^{-3}$ base substitutions/site/year; however, it is not clear whether this value indicates the actual mutation rate of the HCV genome, because complicated quasispecies are generally observed in patients or chimpanzees infected with HCV *in vivo*. On the other hand, Major *et al.* (1999) used chimpanzees that received intrahepatic inoculation with a full-length HCV RNA, and they estimated that the mutation rate of the HCV genome was $1{\cdot}5 \times 10^{-3}$ base substitutions/site/year. However, such experiments on HCV replication in humans are ethically problematic. Thus, there have been few reports on the genetic variations of HCV in an experimental system of HCV replication because of the lack of reproducible and efficient HCV proliferation in cell culture (Kato & Shimotohno, 2000).

In 1999, an HCV replicon system carrying autonomously replicating HCV subgenomic RNA containing the NS3-NS5B regions derived from the strain Con-1 was first established by using a human hepatoma cell line, HuH-7 (Lohmann *et al.*, 1999). Since then, several additional replicon systems have been established (Ali *et al.*, 2004; Blight *et al.*, 2000, 2003; Ikeda *et al.*, 2002; Kato *et al.*, 2003a; Pietschmann *et al.*, 2002; Zhu *et al.*, 2003). In these systems, replicated HCV RNAs were detected by Northern blot analysis and the HCV proteins, which were produced, were detected by Western blot analysis. Therefore, HCV replicon systems are thought to be useful for the analysis of genetic variations and dynamics of HCV.

Recently, we also established two HCV replicons (50-1 and 1B-2R1) derived from two HCV strains, 1B-1 and 1B-2, respectively, using HuH-7 cells (Kato *et al.*, 2003b; Kishine *et al.*, 2002). The nucleotide sequences of the NS3-NS5B regions in the 50-1 replicon showed differences of 8·1 % from those in the 1B-2R1 replicon (Kato *et al.*, 2003b), although both HCV strains belonged to genotype 1b. In order to understand the genetic variations and dynamics of HCV, we performed genetic analysis of HCV replicons obtained in long-term culture of 50-1 and 1B-2R1 replicon cells (termed 50-1 and 1B-2R1 cells, respectively). Here, we show that the accumulation of genetic mutations and the acquisition of the genetic diversity among HCV replicons are time dependent. In addition, we evaluated the effect of ribavirin and mizoribine on the genetic variations and dynamics of HCV replicons.

METHODS

Cell cultures. 50-1 and 1B-2R1 cells were cultured in Dulbecco's modified Eagle's medium supplemented with 10 % fetal bovine serum and 300 μg G418 (Geneticine; Invitrogen) ml^{-1}. The HCV replicon cells were known to possess the G418-resistant phenotype, because neomycin phosphotransferase (Neo^R) was produced by the efficient replication of HCV replicon in the cells. Therefore, when an HCV replicon is excluded from the cells or its level is decreased, the cells are killed by the presence of G418. 50-1 cells were also cultured in the presence of 5 or 25 μM ribavirin (Sigma) or 25 μM mizoribine (Sigma). In general, these replicon cells were passaged every 4 days.

Northern blot analysis. Total RNA from the cultured cells were prepared using an RNeasy extraction kit (Qiagen). Total RNA (3 μg) was used to detect the HCV replicon RNA and β-actin mRNA. Northern blotting and hybridization were performed as described previously (Ikeda *et al.*, 2002; Kato *et al.*, 2003b). A digoxigenin-labelled, negative-sense RNA probe complementary to the NS5B region (positions 8935–9374 of the HCV genome) was used for the detection of the replicon RNA. A β-actin specific digoxigenin-labelled antisense RNA probe was used to check the amount of RNA. The synthetic RNA transcribed from pNSS1RZ2RU (Kato *et al.*, 2003b) (10^8 and 10^7 genome equivalents spiked into normal cellular RNA) was used to compare the level of replicon RNA. An RNA ladder (Invitrogen) was also used to mark the molecular length.

Western blot analysis. The preparation of cell lysates, SDS-PAGE and immunoblotting analysis with a PVDF membrane were performed as described previously (Hijikata *et al.*, 1993; Naganuma *et al.*, 2000). The antibodies used to examine the expression levels of HCV proteins were those against NS3 (Novocastra Laboratories) and NS5B (a generous gift from M. Kohara, Tokyo Metropolitan Institute of Medical Science, Japan). Anti-β-actin antibody (AC-15; Sigma) was also used to detect β-actin as an internal control. Immunocomplexes on the membranes were detected by enhanced chemiluminescence assay (Renaissance; Perkin-Elmer Life Sciences).

RT-PCR. To amplify HCV RNA RT-PCR was performed as described previously (Kato *et al.*, 2003b). Briefly, the total RNA (2 μg) obtained from the replicon cells was used as a template for reverse transcriptase using SuperScript II (Invitrogen). PCR using proofreading KOD-plus DNA polymerase (Toyobo) was performed separately in two parts; one part covered the 5′ UTR to the amino terminal of the NS3 region, and the other part covered the NS3 region to the NS5B region. The PCR yielded a 2033 bp fragment for the former part and a 6107 bp fragment for the latter part.

cDNA cloning and sequencing. The PCR products were subcloned into the *Xba*I site of pBR322MC (Kishine *et al.*, 2002), which was derived from pBR322 and contained the multiple cloning site of pUC19, as described previously (Kato *et al.*, 2003b). Plasmid inserts were sequenced in both the sense and antisense directions by using Big Dye terminator cycle sequencing on an ABI PRISM 310 genetic analyser (Applied Biosystems).

Molecular evolutionary analysis. Nucleotide sequences of the clones obtained by RT-PCRs from 50-1 and 1B-2R1 cells were analysed by the neighbour-joining analysis using the program GENETYX-MAC (Software Development).

RNA transfection and selection of G418-resistant cells. RNA transfection into Huh-7 cells was performed by electroporation as described previously (Lohmann *et al.*, 1999). Briefly, total RNA (80 μg) isolated from the replicon cells was electroporated into 5×10^6 HuH-7 cells, and then 1×10^5 or 3×10^5 cells were seeded into a 10 cm diameter dish. After 48 h, G418 was added to

0·3 mg ml^{-1}, and the medium was changed twice per week. After 3 weeks, the colonies obtained on the culture dish were stained with Coomassie brilliant blue as described previously (Naganuma *et al.*, 2004).

RESULTS

Efficient replication of HCV replicons is maintained in long-term cell culture

In order to prepare the specimens for the genetic analysis of 50-1 and 1B-2R1 replicons, three people independently cultured 50-1 cells; one person cultured for 18 months (M) (K cell culture line; MK) and the two people cultured for 12 months (D and N cell culture lines; MD and MN), and one person cultured 1B-2R1 cells for 12 months. Using the specimens obtained at several time points (after 0, 4, 6, 12 and 18 months in culture), the levels of replicon RNAs and HCV proteins were examined by Northern and Western blot analyses, respectively. As shown in Fig. 1(a), replicon RNAs approximately 8 kb long were detected in all specimens except those from the cured cells, from which the replicons had been eliminated from the replicon cells by treatment with interferon-α. The number of copies of replicon RNAs in total RNA (each 3 μg) extracted from the replicon cells was estimated to be in the range of 10^7 to 10^8 by comparing these replicon RNAs with replicon RNA synthesized *in vitro*. The NS3 and NS5B were also detected in all specimens except those from the cured cells (Fig. 1b). The expression levels of replicon RNAs and HCV proteins differed somewhat among these specimens, and no strong quantitative relationship between replicon RNA and HCV proteins was observed (Fig. 1). These results suggest that the stability of replicon RNA or HCV proteins produced from the replicon RNA, or the efficiency of translation, changes during the periods of cell culture. In summary, we demonstrated that the replication efficiencies of the 50-1 and 1B-2R1 replicons remained high under the G418 selection pressure.

Sequence analysis of the 50-1 and 1B-2R1 replicon RNAs

To clarify the genetic variations and diversities of the replicons during the period of cell culture, we carried out sequence analysis of 50-1 and 1B-2R1 replicon RNAs obtained at several time points in the cultures of both replicon cells. Two separate RNA fragments (one was 2·0 kb in length, containing the 5′ UTR to the amino-terminal of the NS3 region; the other was 6·1 kb in length, containing the NS3 to NS5B regions) were amplified by RT-PCR, and three independent clones of each were sequenced after subcloning into pBR322MC, as described previously (Kato *et al.*, 2003b).

Genetic variations of 50-1 and 1B-2R1 replicons during long-term cell culture

The determined nucleotide sequences of the 50-1 and 1B-2R1 replicon RNAs were compared with those of the

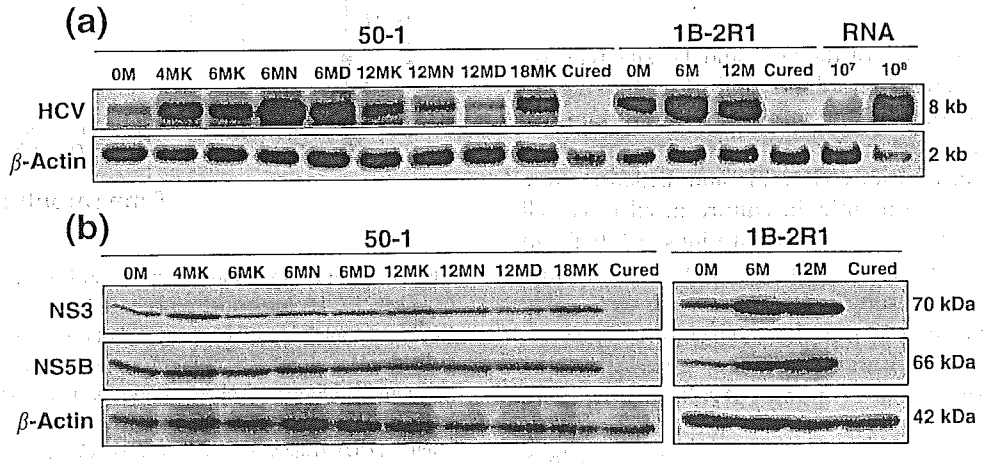

Fig. 1. Characterization of replicon cells in long-term cell culture. (a) Northern blot analysis. Total RNAs from 50-1 cells after 4 months (4MK), 6 months (6MK, 6MN and 6MD), 12 months (12MK, 12MN and 12MD) and 18 months (18MK) in culture, as well as total RNA from the parental 50-1 cells (0M) were used for the analysis. Total RNAs from 1B-2R1 cells after 6 months (6M) and 12 months (12M) in culture, as well as total RNA from the parental 1B-2R1 cells (0M) were used for the analysis. Total RNAs from each cured cells obtained from 50-1 and 1B-2R1 cells by interferon treatment were also used as a negative control. Northern blot analysis was performed using a positive-stranded HCV genome-specific RNA probe (upper panel) and a β-actin-specific probe (lower panel). Synthetic RNA transcribed from pNSS1RZ2RU (10^8 and 10^7 genome equivalents spiked into normal cellular RNA) was used for the comparison of the expression level. (b) Western blot analysis. The orders of specimens were the same as in (a). Productions of NS3 and NS5B in 50-1 and 1B-2R1 cells were analysed by immunoblotting using anti-NS3 and anti-NS5B antibodies, respectively. β-Actin was used as a control for the amount of protein loaded per lane.

original 50-1 (Kishine *et al.*, 2002; GenBank accession no. AB041927) and 1B-2R1 replicons (Kato *et al.*, 2003b; AB109543), respectively. The results revealed that the numbers of base substitutions in the first 2·0 kb region and in the NS region (6·1 kb) of both replicon RNAs were time-dependently increased with linearity (Fig. 2). These substitutions were considered to be mutations that occurred during the intracellular replication of replicon RNA. Based on the results after 12 months in culture, the apparent mutation rates in 50-1 replicon RNA were calculated to be $3{\cdot}1 \times 10^{-3}$ and $3{\cdot}0 \times 10^{-3}$ base substitutions/site/year in the first 2 kb region and NS region, respectively, indicating that there was no difference in mutation rate between the two regions of 50-1 replicon RNA. Interestingly, almost the same mutation rates ($3{\cdot}0 \times 10^{-3}$ base substitutions/site/year in the first 2 kb region; $3{\cdot}1 \times 10^{-3}$ base substitutions/site/year in NS region) were obtained for the 1B-2R1 replicon RNA, suggesting that the replication efficiency of the 1B-2R1 replicon was almost equal to that of the 50-1 replicon.

Fig. 3(a) shows the schematic presentation of mutations detected in the first 2 kb region by comparison with the original sequences (NNRZ2RU) of 50-1 and 1B-2R1 replicon RNAs (Kato *et al.*, 2003b; Kishine *et al.*, 2002). The results revealed that there were no common mutations among the four cell culture lines (three for 50-1 and one for 1B-2R1) over at least 12 months of cell culture. However, genetic mutations in both replicons were time-dependently increased and accumulated, and several mutations became abundant during the subsequent cell culture (Fig. 3a).

The NS regions (6·1 kb) of the 50-1 and 1B-2R1 replicon RNAs were also analysed in addition to the first 2 kb region. The mutation sites that showed amino acid substitutions are schematically presented in Fig. 3(b). Regarding the 50-1 replicon, 2 aa substitutions (P1115L and E1966A) were newly detected after 6 months in culture in all three cell culture lines, in addition to 2 aa substitutions (K1609E and V1896F) already observed when the replicon was first established. These four substituted amino acids were stably maintained over at least 12 months of cell culture. However, such amino acid substitutions were not observed in the 1B-2R1 replicon even after 12 months of culture. After more than 12 months in culture, several culture line-specific amino acid substitutions (*1–5 for the K culture line; *6–8 for the D culture line; and *9–12 for the N culture line in Fig. 3b) were observed in the 50-1 replicon. Also in the 1B-2R1 replicon, 1 aa substitution (*13 in Fig. 3b) was detected after 12 months in culture; however, no common amino acid substitutions were observed between the 50-1 and 1B-2R1 replicons. The mean numbers of amino acid substitutions occurring after 6 and 12 months in culture were 4·2 and 8·9, respectively, for the 50-1 replicon, and 4·7 and 10·0, respectively, for the 1B-2R1 replicon. These values indicate a steady genetic evolution of 50-1 and 1B-2R1 replicons during the cell culture.

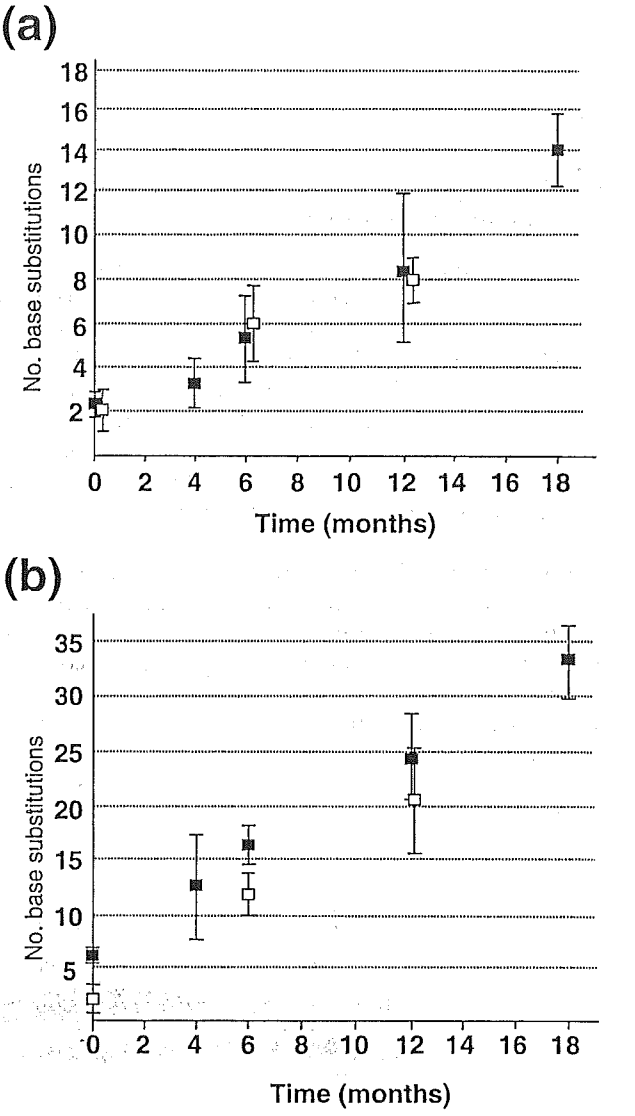

Fig. 2. Genetic variations of 50-1 and 1B-2R1 replicon RNAs. (a) First 2·0 kb region of replicon RNA. Filled squares indicate the mean numbers of base substitutions detected in nine (after 0, 6 and 12 months in culture) or three (after 4 and 18 months in culture) clones containing the first 2·0 kb region of 50-1 replicon RNA, by comparison with its original sequences (NNRZ2RU) (Kishine *et al.*, 2002). Open squares indicate the mean numbers of base substitutions detected in three clones containing the first 2·0 kb region of 1B-2R1 replicon RNA, by comparison with its original sequences (NNRZ2RU) (Kishine *et al.*, 2002). (b) NS region (6·1 kb) of replicon RNA. Filled squares indicate the mean numbers of base substitutions detected in nine (after 0, 6 and 12 months in culture) or three (after 4 and 18 months in culture) clones containing the NS region of 50-1 replicon RNA, by comparison with its original sequences (Kishine *et al.*, 2002). Open squares indicate the mean numbers of base substitutions detected in three clones containing the NS region of 1B-2R1 replicon RNA, by comparison with its original sequences (Kato *et al.*, 2003b).

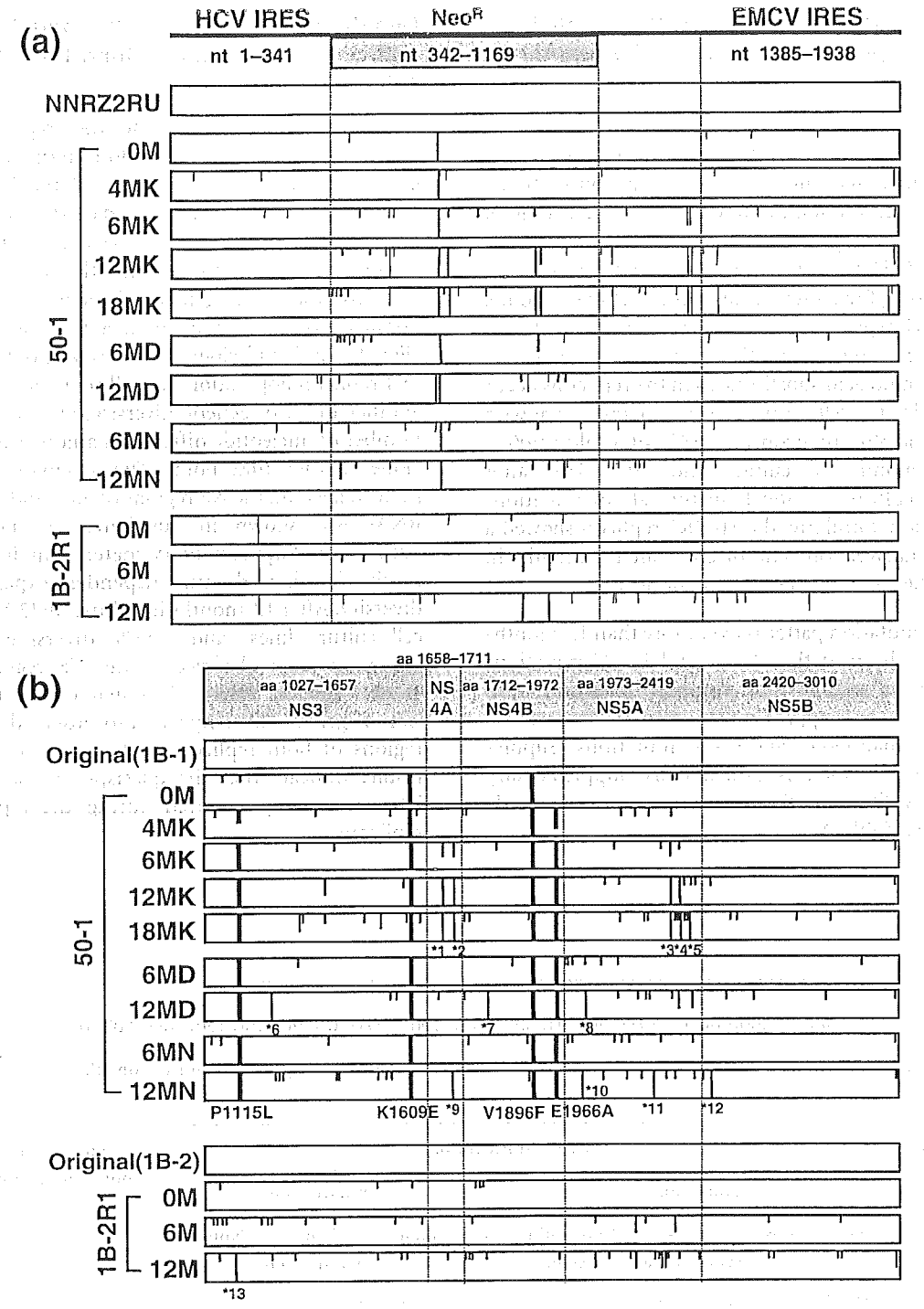

Fig. 3. Genetic variations of 50-1 and 1B-2R1 replicons in long-term cell culture. (a) Schematic presentation of mutations detected in first 2·0 kb regions of the replicon RNAs. Compared with the nucleotide sequences of the first 2·0 kb region of the original replicon RNA (NNRZ2RU), nucleotide positions mutated in all three clones, in two of three clones and in one of three clones are indicated by full-length, two-thirds and one-third vertical lines, respectively. Non-synonymous substitutions in the Neo^R region are indicated by heavy vertical lines. (b) Schematic presentation of amino acid substitutions detected in the NS regions of the replicons. Compared with the amino acid sequences of NS region of the original 50-1 (Kishine *et al.*, 2002) and 1B-2R1 replicons (Kato *et al.*, 2003b), amino acid positions substituted in all three clones, in two of three clones and in one of three clones are indicated by full-length, two-thirds and one-third vertical lines, respectively. Four amino acid substitutions (P1115L, K1609E, V1896F and E1966A) are indicated by heavy vertical lines. Culture line-specific amino acid substitutions (indicated by the numbers with asterisks) are as follows: *1, I1686V; *2, L1701R; *3, T2332A; *4, G2336E; *5, A2372T; *6, A1243G; *7, I1797V; *8, S2053G; *9, L1701R; *10, T2051N; *11, R2279G; *12, L2476M; *13, I1097V.

Classification of mutations occurring in 50-1 and 1B-2R1 replicon RNAs during the long-term cell culture

To understand the mutation mode of the replicons in long-term cell culture, we examined the numbers of synonymous and non-synonymous mutations with transition or transversion. The results are summarized in Table 1. The ratio of synonymous to non-synonymous mutations in 50-1 replicon RNA was 0·81 to 1·50 (1·38±0·14 after 6 months in culture and 1·03±0·20 after 12 months in culture), and the ratio in 1B-2R1 replicon RNA was 0·63 after 6 months in culture and 0·59 after 12 months in culture. These values indicate that amino acid substitutions in the replicons occur frequently during the cell culture. The rate of mutations with transition in the 50-1 replicon was 1·82–4·06-fold (2·00±0·18 after 6 months in culture and 2·85±1·07 after 12 months in culture) greater than the rate of mutations with transversion. Similarly, the 1B-2R1 replicon showed a transition-to-transversion ratio of 2·69 (after 6 months in culture) or 2·86 (after 12 months in culture).

Regarding the mutation patterns over more than 12 months of culture, we observed that A→G and U→C mutations were the most and second-most common mutations, and these mutations were approximately two to three times more common than G→A and C→U mutations (Supplementary Table A, which is available as Supplementary material in JGV Online). The rarest mutation was G→U (Supplementary Table A).

Genetic diversity of the 50-1 and 1B-2R1 replicons arising during long-term cell culture

To clarify whether or not the replicons acquire a quasispecies nature during long-term cell culture, we estimated the genetic diversities of the 50-1 and 1B-2R1 replicon populations. First, based on the sequence data of all clones obtained in this study, we constructed phylogenetic trees for the first 2 kb region and the NS region. The results revealed that the genetic diversity of 50-1 replicon populations was expanded in a time-dependent manner (Fig. 4). Similar phylogenetic trees were obtained for the 1B-2R1 replicon populations as well (data not shown). Next, as another index of genetic diversity, we calculated the mean number of nucleotide differences among three independent clones at each time point. The schematic presentation of such analysis on the NS regions of 50-1 and 1B-2R1 replicon RNAs was shown in Supplementary Fig. A, which is available as Supplementary material in JGV Online. The results also showed a time-dependent expansion of genetic diversity. After 12 months in culture, 0·32 % (mean of three cell culture lines) and 0·55 % diversities in nucleotide sequences were observed in the NS region of 50-1 and 1B-2R1 replicon RNAs. A similar time-dependent expansion of genetic diversity was also observed in the first 2 kb regions of both replicon RNAs (data not shown). These results indicate that the quasispecies nature of replicon RNA was easily acquired during the replication of the replicons.

Table 1. Base substitutions occurring in 50-1 and 1B-2R1 replicon RNAs during long-term cell culture

The counting of base substitutions was performed by comparison with the consensus sequence obtained from the 0M series of 50-1 or 1B-2R1 replicon.

Replicon	series	No. base substitutions										Synonymous/ non-synonymous	Transition/ transversion
		Transition					Transversion						
		Synonymous		Non-synonymous		Non-coding region	Synonymous		Non-synonymous		Non-coding region		
		Neo^R	NS	Neo^R	NS		Neo^R	NS	Neo^R	NS			
50-1	4MK	1	13	0	8	4	0	5	0	6	2	1·36	2·00
	6MK	0	20	2	10	8	3	8	1	9	1	1·41	1·82
	12MK	3	29	6	19	13	4	9	4	9	2	1·18	2·50
	18MK	5	43	8	26	16	3	10	4	14	5	1·17	2·72
	6MD	3	20	3	9	2	0	5	4	7	1	1·22	2·18
	12MD	5	29	2	26	3	2	5	1	8	0	1·11	4·06
	6MN	2	19	2	8	3	2	4	0	8	3	1·50	2·00
	12MN	3	25	2	21	9	1	6	5	15	3	0·81	2·00
1B-2R1	6M	1	14	5	14	1	1	1	3	5	3	0·63	2·69
	12M	2	22	4	29	6	1	2	3	10	6	0·59	2·86

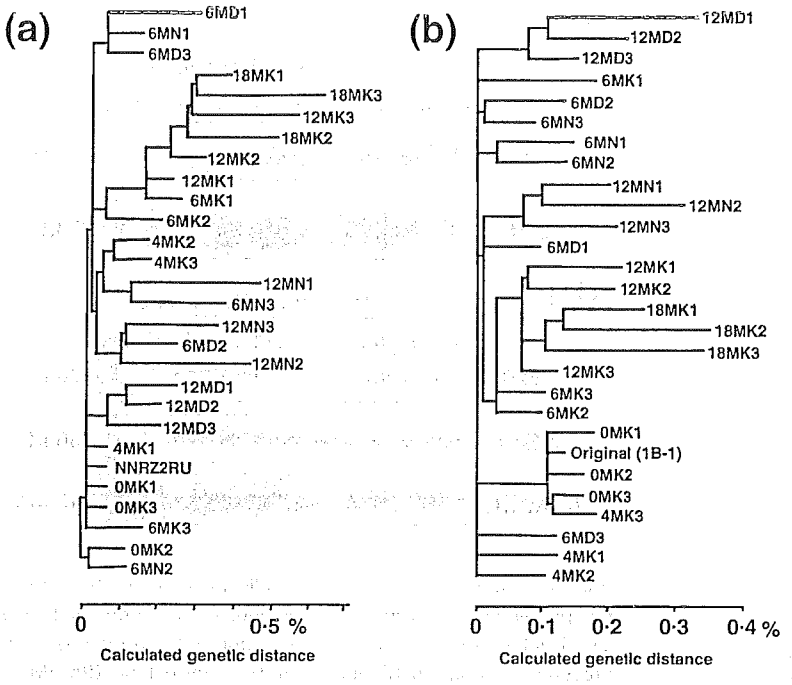

Fig. 4. Phylogenetic trees of 50-1 replicon populations obtained in long-term cell culture. The phylogenetic tree is depicted on the basis of nucleotide sequences of all replicon clones obtained by long-term culture of 50-1 cells. (a) The first 2·0 kb region of replicon RNA. NNRZ2RU indicates the original sequences of 50-1 replicon RNA, and the others indicate the names of clones. (b) The NS region of replicon RNA. Original (1B-1) indicates the original sequences of 50-1 replicon RNA, and the others indicate the names of clones.

Enhancement of HCV replication is associated with the expansion of the replicons' genetic diversity

To assess whether or not the mutations accumulating in the replicons increase the replication efficiencies of the replicons, the efficiency of colony formation (ECF) of the replicon was examined at each time point of the culture. An ECF assay was performed by transfection of total RNAs isolated from 50-1 and 1B-2R1 replicon cells at different time points into naïve HuH-7 cells. After 3 weeks of G418 selection, only a few colonies were obtained when RNAs from 50-1 replicon cells cultured less than 4 month were used (Fig. 5). However, ECF was apparently increased when RNAs from cells cultured 6 months, in particular the D and N cell culture lines, were used, and much higher numbers of colonies were obtained when RNAs from cells cultured 12 months were used (Fig. 5). Interestingly, ECFs of RNAs from D and N cell lines cultured more than 6 months were higher than those in the K cell culture line. These results indicated that ECF of the replicon was increased with the cultured periods of the replicon cells and suggested that ECF enhancement is associated with the expansion of the 50-1 replicon's genetic diversity.

In contrast to the case with 50-1 replicon cells, a number of colonies were obtained even when RNA from the initial culture of 1B-2R1 replicon cells was used (Fig. 5). In this replicon also, the ECF of RNA from cells cultured 12 months was apparently higher than those of RNA from the initial culture or 6 months of culture (Fig. 5). These results suggest that S2200R substitution, which was detected when the 1B-2R1 replicon was established (Kato *et al.*, 2003b), function as an adaptive mutation, and that the expansion of genetic diversity in the 1B-2R1 replicon also contributes to the enhancement of ECF, as was the case with the 50-1 replicon.

Effect of ribavirin and mizoribine on the genetic evolution and dynamics of the 50-1 replicon

Combined treatment of interferon plus ribavirin for patients with chronic hepatitis C has been shown to be more effective than treatment with interferon alone (McHutchison *et al.*, 1998), although it has been shown that ribavirin alone does not cause a decrease of HCV level in patients with chronic hepatitis C. Recently, several groups have reported that ribavirin might cause 'error catastrophe' of HCV genome (Contreras *et al.*, 2002; Tanabe *et al.*, 2004; Zhou *et al.*, 2003), however, controversial results have also been reported (Schinkel *et al.*, 2003). Therefore, to clarify whether or not ribavirin affects the genetic alterations of HCV, we cultured parent 50-1 cells (corresponding to 0M in Fig. 1) for 6 months in the presence of ribavirin (5 or 25 μM) or its derivative molecule, mizoribine (25 μM). As a control, the parent 50-1 cells were also cultured for 6 months in the absence of ribavirin or mizoribine. After 6 months in culture, the levels of replicon RNAs and HCV proteins were examined by Northern and Western blot analyses, respectively. As shown in Fig. 6(a), the level of replicon RNA in the cells treated with ribavirin or mizoribine was almost the same as that in the cells without ribavirin or mizoribine treatment. The NS3 and NS5B were also expressed at similar levels in the cells irrespective of ribavirin or mizoribine treatment (Fig. 6b). These results indicate that even 6 months of treatment with ribavirin or mizoribine did not prevent the replication of replicon RNA under the G418 selection pressure. Using the 50-1 cells cultured for 6 months with or without ribavirin or mizoribine, we performed sequence analysis of replicon

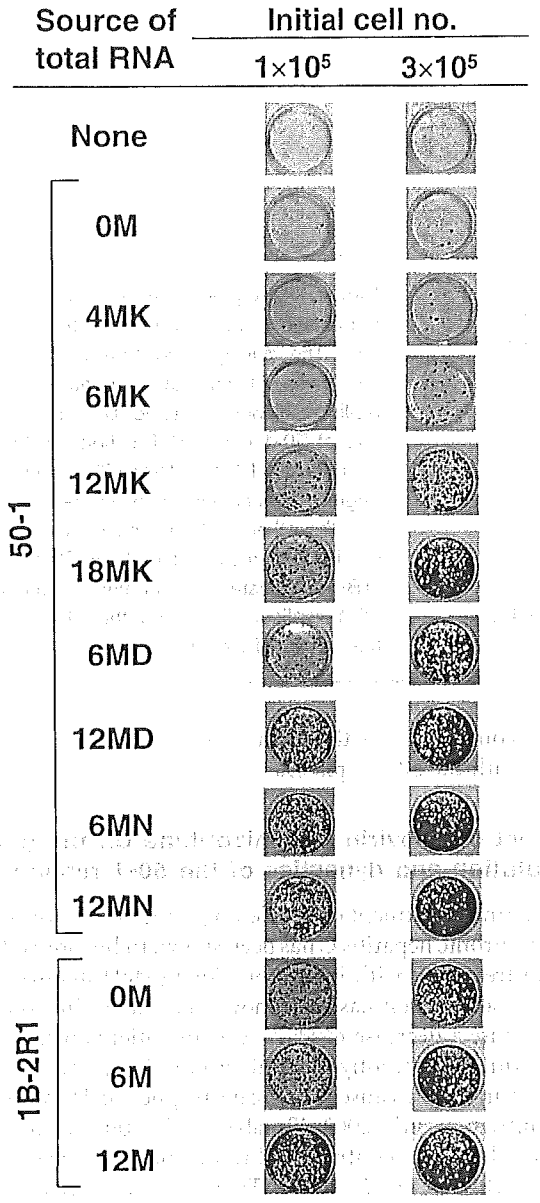

Fig. 5. ECF of the RNAs isolated from 50-1 and 1B-2R1 replicon cells at different time points in the culture. Total RNAs obtained from the replicon cells were transfected into HuH-7 cells as described in Methods. The panels show the cell colonies that were recovered after 3 weeks of G418 selection.

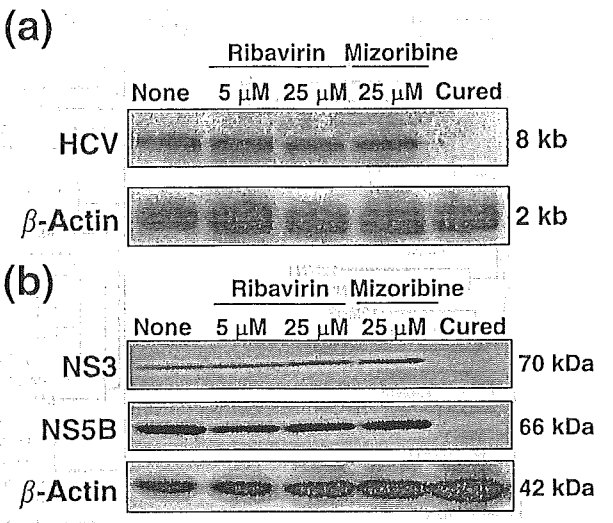

Fig. 6. Characterization of 50-1 cells cultured for 6 months in the presence of ribavirin or mizoribine. (a) Northern blot analysis. Total RNAs from 50-1 cells cultured for 6 months in the presence of ribavirin (5 and 25 μM) or mizoribine (25 μM), as well as total RNA from 50-1 cells cultured for 6 months in the absence of ribavirin and mizoribine were used for the analysis. Northern blot analysis was performed as indicated in Fig. 1(a). (b) Western blot analysis. The orders of specimens were the same as in (a). Western blot analysis was performed as indicated in Fig. 1(b).

RNAs as described above. As shown in Table 2, the results revealed that the numbers of mutations in the first 2·0 kb and NS regions of the replicon RNAs sequenced were not significantly different among the specimens, although the number in the NS region derived from the cells treated with 25 μM of ribavirin was a little lower than those of the other specimens. These results suggest that the treatment of replicon cells with either ribavirin or mizoribine does not increase the mutation rate of replicon RNA. The ratio of synonymous and non-synonymous mutations, and the ratio of transition and transversion mutations were also not altered by ribavirin or mizoribine treatment (data not shown). In addition, we did not observe any ribavirin- or mizoribine-specific common amino acid substitutions in either the first 2 kb or NS regions of the replicon RNA, although P1115L and E1966A were detected after 6 months in culture in all cell culture lines. The above-described analysis of genetic diversity among the replicon RNAs did

Table 2. Base substitutions occurred in 50-1 replicon RNA during 6 months culture in the presence of ribavirin or mizoribine

6MR5 and 6MR25 indicate the series treated with 5 and 25 μM of ribavirin, respectively. 6MM25 indicates the series treated with 25 μM of mizoribine. The counting of base substitutions was performed by the comparison with the original sequence of 50-1 replicon (Kishine *et al.*, 2002).

Series	First 2-kb region	NS region
6M (Fig. 2)	5·4±1·9*	16·4±1·8
6M	5·7±2·5	16·0±0·0
6MR5	5·7±1·5	16·3±1·5
6MR25	5·7±1·5	10·7±1·2
6MM25	3·7±0·6	18·7±4·0

*Numbers of base substitutions ± SD.

not reveal any significant differences between the specimens derived from the replicon cells with and those without ribavirin or mizoribine treatment (data not shown). Taken together, these results suggest that neither ribavirin nor mizoribine accelerated the mutation rate of HCV replicons or the development of their quasispecies nature.

DISCUSSION

In this study, we analysed the genetic evolution and dynamics of HCV replicons, and time-dependent genetic mutations of HCV replicons were observed. Time-dependent expansions of their genetic diversities were also revealed. Our results should provide useful fundamental information for understanding the remarkable genetic diversity and variation among the HCV genomes observed in patients with chronic hepatitis C.

Although RT-PCR techniques were used to amplify the replicon RNAs in this study, it is unlikely that the detected mutations were due to errors related to the use of the KOD-plus DNA polymerase in the PCR reaction, because we previously showed that KOD-plus DNA polymerase possessed a high proofreading activity (Alam *et al.*, 2002; Naganuma *et al.*, 2004). Furthermore, in the present study, we sequenced several clones (containing a 2·0 or 6·1 kb fragment) obtained by PCR using KOD-plus DNA polymerase and a single sequenced clone as a template, but no mutations were detected in these sequenced clones, indicating that KOD-plus DNA polymerase possesses extremely high fidelity. However, we are not able to completely exclude the possibility that some substitutions resulted from the erroneous use of KOD-plus DNA polymerase during the PCR. Even if such errors occurred, the error frequency is estimated to be less than one nucleotide per sequenced clone. This is explained as follows. Fig. 2 shows that the numbers of substitutions time-dependently increased with linearity in both HCV replicons. Interestingly, when these linear lines are extrapolated to zero base substitutions, the crossing points show approximately −2–−3 months in the time axis. These range of months is in accord with the time of initial electroporation of HCV replicon RNA to HuH-7 cells. Therefore, PCR-induced mutations are considered to be very rare and such mutations would have very little effect on the results shown in Fig. 2. In addition, to avoid a sampling effect, we sequenced three independent clones derived from each time point.

We showed that the mutation rates for the 50-1 and 1B-2R1 replicon RNAs were almost the same – about 3×10^{-3} base substitutions/site/year. However, the actual mutation frequency of the replicon RNAs would be higher than this value, because the mutations that occurred in positions that were critical for the replication of replicon RNA should not have been passed on to the progeny. Our observed mutation rates of the replicon RNAs were approximately two times higher than those previously obtained in chimpanzees and clinical patients with chronic hepatitis C (Major *et al.*, 1999; Ogata *et al.*, 1991; Okamoto *et al.*, 1992). Since the selective pressure of the immune system also functions *in vivo* (Kato *et al.*, 1993), the mutation rate in cell culture obtained in this study may be reasonable value as a potential mutation rate of HCV. However, direct comparison of these mutation rates would be difficult, because both the experimental model and analytical method were different in this study compared with the previous studies. It would be interesting to examine whether this mutation rate (3×10^{-3} base substitutions/site/year) would be maintained during longer-term culture of the replicon cells. If so, approximately 3 % of nucleotide sequences of the replicon RNAs might be mutated after 10 years in cell culture. Alternatively, the mutations might become saturated during further long-term culture of the replicon cells. To clarify this point, further long-term culture of replicon cells is in progress.

Although the mutations detected in this study were dispersed throughout the entire length of the replicon RNAs (Fig. 3), the mutation frequencies in the 5′ UTR and NS5B region were lower than those in other regions, and the NS5A region showed the highest mutation frequency. These observations are consistent with the genetic diversities of HCVs in patients with chronic hepatitis C reported to date (Kato, 2001). In addition, the positions in which amino acid substitutions were observed during the cell culture did not appear to be critical for replication of the HCV genome.

Time-dependent expansions of genetic diversities of HCV replicons were also found in this study. However, this finding seems to be different from the previous findings that HCV populations in the cells infected *in vitro* gradually altered with time and converged to the limited populations (Kato *et al.*, 1998; Kato, 2001). This gap may have been due to the differences in the HCV sources used: a patient's inoculum containing a quasispecies of HCV was used for the *in vitro* infection experiment, and a single HCV species was used for the replicon system. Alternatively, the gap may have been due to the overwhelming difference between the replication level of the HCV genome in the cells infected *in vitro* and that in the replicon cells.

To date, a number of amino acid substitutions belonging to adaptive mutations that enhance the frequency with which the replicon is established *in vitro* have been found in established HCV replicons (Bartenschlager, 2002; Blight *et al.*, 2000, 2003; Ikeda *et al.*, 2002; Krieger *et al.*, 2001; Lanford *et al.*, 2003; Lohmann *et al.*, 2001, 2003; Pflugheber *et al.*, 2002). Although none of the amino acid substitutions detected in the long-term cultures of the 50-1 and 1B-2R1 replicons were the same as those reported as adaptive mutations, ECF analysis of the replicons using naïve HuH-7 cells suggested that adaptive mutations accumulated in the replicon populations in a time-dependent manner. In particular, drastic enhancement of ECF was observed in the 50-1 replicon after 6 months of culture. However, this result suggests that the four common amino acid substitutions (P1115L, K1609E, V1896F and E1966A) do not contribute much to the drastic enhancement of ECF,

because the ECFs of 4MK and 6MK samples possessing these substitutions did not increase much. Therefore, we estimate that some uncommon amino acid substitutions accumulated as so-called adaptive mutations. The candidates for such adaptive mutations are culture-line-specific amino acid substitutions (Fig. 3b, *1–12), and many amino acid substitutions sporadically appeared in the replicons in the long-term cell cultures. To identify which amino acid substitution is the main contributor to the drastic enhancement of ECF, further transfection experiments using replicon RNAs possessing mutations will be needed. Based on the results of this study, S2200R substitution in the 1B-2R1 replicon is considered an adaptive mutation. This description is supported by the previous result that we were unable to obtain any G418-resistant colonies when the original 1B-2 replicon RNA library, used in the isolation of the 1B-2R1 replicon, was transfected into naïve HuH-7 cells (Kato *et al.*, 2003b). Since the ECF of 1B-2R1 replicon RNA from 12 months of culture was further enhanced, it may be that the I1097V substitution, detected commonly at 12 months of culture, functions as an additional adaptive mutation.

Interestingly, once a new mutation was observed in all three clones at a particular time point, the clones which went back to the original sequences were never obtained in the subsequent cell culture, except for one clone (a mutation in the HCV IRES region) derived from 1B-2R1 replicon cells after 12 months in culture (Fig. 3a). This finding suggests that the genetic evolution of HCV replicons is irreversibly progressing.

Although the mechanism of action of ribavirin for patients with chronic hepatitis C is ambiguous, an 'error catastrophe' theory of ribavirin has been proposed by several groups (Contreras *et al.*, 2002; Tanabe *et al.*, 2004; Zhou *et al.*, 2003). However, our results obtained in this study were not able to support this 'error catastrophe' theory, because ribavirin had no effect on the genetic variation and diversity of the 50-1 replicon. The concentration (5 and 25 μM) of ribavirin used in this study was considered to be reasonable, because the growth rate of 50-1 cells decreased at a ribavirin concentration of more than 50 μM, and approximately 10 μM of ribavirin is the maximum plasma concentration in current clinical usage (Tanabe *et al.*, 2004). Higher concentration (more than 50 μM) of ribavirin used in previous studies may be required for causation of the error catastrophe. Recently, a single amino acid substitution (F2834Y) was identified as a ribavirin-resistant NS5B mutation in genotype 1a (Young *et al.*, 2003); however, it is difficult to evaluate that finding in this study, because most of the HCV strains belonging to genotype 1b, including 1B-1 (50-1) and 1B-2 (1B-2R1), already possess a Tyr residue at position 2834. No amino acid substitution at position 2834 in NS5B was observed in the replicon cells treated with ribavirin.

This study provided the fact that the genetic diversity of HCV replicons was enlarged in a time-dependent manner during long-term cell culture. Since all the HCV replicons established to date have been shown to be highly sensitive to interferon-α, -β and -γ (Kato *et al.*, 2003b), and most of the HCV replicons established to date are able to replicate in only HuH-7 cells, the extensive genetic polymorphism of HCV replicon populations obtained by long-term cell culture may change the sensitivity against interferon or the ability of replication in the cells except for HuH-7. In the future, it will be necessary to clarify these points. Thus, HCV replicon populations obtained by long-term cell culture may be useful not only for analysis of the genetic variations and dynamics of HCV but also for analysis of the variable properties of HCV.

ACKNOWLEDGEMENTS

This work was supported by grants-in-aid for research on hepatitis from the Ministry of Health, Labour and Welfare of Japan and by grants-in-aid for scientific research from the Organization for Pharmaceutical Safety and Research (OPSR).

REFERENCES

Alam, S. S., Nakamura, T., Naganuma, A., Nozaki, A., Nouso, K., Shimomura, H. & Kato, N. (2002). Hepatitis C virus quasispecies in cancerous and noncancerous hepatic lesions: the core protein-encoding region. *Acta Med Okayama* 56, 141–147.

Ali, S., Pellerin, C., Lamarre, D. & Kukolj, G. (2004). Hepatitis C virus subgenomic replicons in the human embryonic kidney 293 cell line. *J Virol* 78, 491–501.

Bartenschlager, R. (2002). Hepatitis C virus replicons: potential role for drug development. *Nat Rev Drug Discov* 1, 911–916.

Bartenschlager, R. & Lohmann, V. (2000). Replication of hepatitis C virus. *J Gen Virol* 81, 1631–1648.

Blight, K. J., Kolykhalov, A. A. & Rice, C. M. (2000). Efficient initiation of HCV RNA replication in cell culture. *Science* 290, 1972–1974.

Blight, K. J., McKeating, J. A., Marcotrigiano, J. & Rice, C. M. (2003). Efficient replication of hepatitis C virus genotype 1a RNAs in cell culture. *J Virol* 77, 3181–3190.

Bukh, J., Miller, R. H. & Purcell, R. H. (1995). Genetic heterogeneity of hepatitis C virus: quasispecies and genotypes. *Semin Liver Dis* 15, 41–63.

Choo, Q. L., Kuo, G., Weiner, A. J., Overby, L. R., Bradley, D. W. & Houghton, M. (1989). Isolation of a cDNA clone derived from a blood-borne non-A, non-B viral hepatitis genome. *Science* 244, 359–362.

Contreras, A. M., Hiasa, Y., He, W., Terella, A., Schmidt, E. V. & Chung, R. T. (2002). Viral RNA mutations are region specific and increased by ribavirin in a full-length hepatitis C virus replication system. *J Virol* 76, 8505–8517.

Grakoui, A., Wychowski, C., Lin, C., Feinstone, S. M. & Rice, C. M. (1993). Expression and identification of hepatitis C virus polyprotein cleavage products. *J Virol* 67, 1385–1395.

Hijikata, M., Kato, N., Ootsuyama, Y., Nakagawa, M. & Shimotohno, K. (1991). Gene mapping of the putative structural region of the hepatitis C virus genome by *in vitro* processing analysis. *Proc Natl Acad Sci U S A* 88, 5547–5551.

Hijikata, M., Mizushima, H., Tanji, Y., Komoda, Y., Hirowatari, Y., Akagi, T., Kato, N., Kimura, K. & Shimotohno, K. (1993). Proteolytic processing and membrane association of putative nonstructural proteins of hepatitis C virus. *Proc Natl Acad Sci U S A* 90, 10773–10777.

Ikeda, M., Yi, M., Li, K. & Lemon, S. M. (2002). Selectable subgenomic and genome-length dicistronic RNAs derived from an infectious molecular clone of the HCV-N strain of hepatitis C virus replicate efficiently in cultured Huh7 cells. *J Virol* 76, 2997–3006.

Kato, N. (2001). Molecular virology of hepatitis C virus. *Acta Med Okayama* 55, 133–159.

Kato, N. & Shimotohno, K. (2000). Systems to culture hepatitis C virus. *Curr Top Microbiol Immunol* 242, 261–278.

Kato, N., Hijikata, M., Ootsuyama, Y., Nakagawa, M., Ohkoshi, S., Sugimura, T. & Shimotohno, K. (1990a). Molecular cloning of the human hepatitis C virus genome from Japanese patients with non-A, non-B hepatitis. *Proc Natl Acad Sci U S A* 87, 9524–9528.

Kato, N., Hijikata, M., Ootsuyama, Y., Nakagawa, M., Ohkoshi, S. & Shimotohno, K. (1990b). Sequence diversity of hepatitis C viral genomes. *Mol Biol Med* 7, 495–501.

Kato, N., Ootsuyama, Y., Tanaka, T., Nakagawa, M., Nakazawa, T., Muraiso, K., Ohkoshi, S., Hijikata, M. & Shimotohno, K. (1992). Marked sequence diversity in the putative envelope proteins of hepatitis C viruses. *Virus Res* 22, 107–123.

Kato, N., Sekiya, H., Ootsuyama, Y., Nakazawa, T., Hijikata, M., Ohkoshi, S. & Shimotohno, K. (1993). Humoral immune response to hypervariable region 1 of the putative envelope glycoprotein (gp70) of hepatitis C virus. *J Virol* 67, 3923–3930.

Kato, N., Ikeda, M., Sugiyama, K., Mizutani, T., Tanaka, T. & Shimotohno, K. (1998). Hepatitis C virus population dynamics in human lymphocytes and hepatocytes infected in vitro. *J Gen Virol* 79, 1859–1869.

Kato, T., Date, T., Miyamoto, M., Furusaka, A., Tokushige, K., Mizokami, M. & Wakita, T. (2003a). Efficient replication of the genotype 2a hepatitis C virus subgenomic replicon. *Gastroenterology* 125, 1808–1817.

Kato, N., Sugiyama, K., Namba, K., Dansako, H., Nakamura, T., Takami, M., Naka, K., Nozaki, A. & Shimotohno, K. (2003b). Establishment of a hepatitis C virus subgenomic replicon derived from human hepatocytes infected in vitro. *Biochem Biophys Res Commun* 306, 756–766.

Kishine, H., Sugiyama, K., Hijikata, M. & 7 other authors (2002). Subgenomic replicon derived from a cell line infected with the hepatitis C virus. *Biochem Biophys Res Commun* 293, 993–999.

Krieger, N., Lohmann, V. & Bartenschlager, R. (2001). Enhancement of hepatitis C virus RNA replication by cell culture-adaptive mutations. *J Virol* 75, 4614–4624.

Kuo, G., Choo, Q. L., Alter, H. J. & 17 other authors (1989). An assay for circulating antibodies to a major etiologic virus of human non-A, non-B hepatitis. *Science* 244, 362–364.

Lanford, R. E., Guerra, B., Lee, H., Averett, D. R., Pfeiffer, B., Chavez, D., Notvall, L. & Bigger, C. (2003). Antiviral effect and virus-host interactions in response to alpha interferon, gamma interferon, poly(i)-poly(c), tumor necrosis factor alpha, and ribavirin in hepatitis C virus subgenomic replicons. *J Virol* 77, 1092–1104.

Lohmann, V., Korner, F., Koch, J., Herian, U., Theilmann, L. & Bartenschlager, R. (1999). Replication of subgenomic hepatitis C virus RNAs in a hepatoma cell line. *Science* 285, 110–113.

Lohmann, V., Korner, F., Dobierzewska, A. & Bartenschlager, R. (2001). Mutations in hepatitis C virus RNAs conferring cell culture adaptation. *J Virol* 75, 1437–1449.

Lohmann, V., Hoffmann, S., Herian, U., Penin, F. & Bartenschlager, R. (2003). Viral and cellular determinants of hepatitis C virus RNA replication in cell culture. *J Virol* 77, 3007–3019.

Major, M. E., Mihalik, K., Fernandez, J., Seidman, J., Kleiner, D., Kolykhalov, A. A., Rice, C. M. & Feinstone, S. M. (1999). Long-term follow-up of chimpanzees inoculated with the first infectious clone for hepatitis C virus. *J Virol* 73, 3317–3325.

Martell, M., Esteban, J. I., Quer, J., Genesca, J., Weiner, A., Esteban, R., Guardia, J. & Gomez, J. (1992). Hepatitis C virus (HCV) circulates as a population of different but closely related genomes: quasispecies nature of HCV genome distribution. *J Virol* 66, 3225–3229.

McHutchison, J. G., Gordon, S. C., Schiff, E. R. & 7 other authors (1998). Interferon alfa-2b alone or in combination with ribavirin as initial treatment for chronic hepatitis C. Hepatitis Interventional Therapy Group. *N Engl J Med* 339, 1485–1492.

Mizushima, H., Hijikata, M., Tanji, Y., Kimura, K. & Shimotohno, K. (1994). Analysis of N-terminal processing of hepatitis C virus nonstructural protein 2. *J Virol* 68, 2731–2734.

Naganuma, A., Nozaki, A., Tanaka, T., Sugiyama, K., Takagi, H., Mori, M., Shimotohno, K. & Kato, N. (2000). Activation of the interferon-inducible 2′-5′-oligoadenylate synthetase gene by hepatitis C core protein. *J Virol* 74, 8744–8750.

Naganuma, A., Dansako, H., Nakamura, T., Nozaki, A. & Kato, N. (2004). Promotion of microsatellite instability by hepatitis C virus core protein in human non-neoplastic hepatocyte cells. *Cancer Res* 64, 1307–1314.

Ogata, N., Alter, H. J., Miller, R. H. & Purcell, R. H. (1991). Nucleotide sequence and mutation rate of the H strain of hepatitis C virus. *Proc Natl Acad Sci U S A* 88, 3392–3396.

Ohkoshi, S., Kojima, H., Tawaraya, H. & 8 other authors (1990). Prevalence of antibody against non-A, non-B hepatitis virus in Japanese patients with hepatocellular carcinoma. *Jpn J Cancer Res* 81, 550–553.

Okamoto, H., Kojima, M., Okada, S. & 7 other authors (1992). Genetic drift of hepatitis C virus during an 8·2-year infection in a chimpanzee: variability and stability. *Virology* 190, 894–899.

Pflugheber, J., Fredericksen, B., Sumpter, R., Jr, Wang, C., Ware, F., Sodora, D. L. & Gale, M., Jr (2002). Regulation of PKR and IRF-1 during hepatitis C virus RNA replication. *Proc Natl Acad Sci U S A* 99, 4650–4655.

Pietschmann, T., Lohmann, V., Kaul, A., Krieger, N., Rinck, G., Rutter, G., Strand, D. & Bartenschlager, R. (2002). Persistent and transient replication of full-length hepatitis C virus genomes in cell culture. *J Virol* 76, 4008–4021.

Saito, I., Miyamura, T., Ohbayashi, A. & 10 other authors (1990). Hepatitis C virus infection is associated with the development of hepatocellular carcinoma. *Proc Natl Acad Sci U S A* 87, 6547–6549.

Schinkel, J., de Jong, M. D., Bruning, B., van Hoek, B., Spaan, W. J. & Kroes, A. C. (2003). The potentiating effect of ribavirin on interferon in the treatment of hepatitis C: lack of evidence for ribavirin-induced viral mutagenesis. *Antivir Ther* 8, 535–540.

Simmonds, P. (1995). Variability of hepatitis C virus. *Hepatology* 21, 570–583.

Tanabe, Y., Sakamoto, N., Enomoto, N. & 9 other authors (2004). Synergistic inhibition of intracellular hepatitis C virus replication by combination of ribavirin and interferon-alpha. *J Infect Dis* 189, 1129–1139.

Tanaka, T., Kato, N., Nakagawa, M., Ootsuyama, Y., Cho, M. J., Nakazawa, T., Hijikata, M., Ishimura, Y. & Shimotohno, K. (1992). Molecular cloning of hepatitis C virus genome from a single

Japanese carrier: sequence variation within the same individual and among infected individuals. *Virus Res* 23, 39–53.

Tanaka, T., Kato, N., Cho, M. J. & Shimotohno, K. (1995). A novel sequence found that at the 3′ terminus of hepatitis C virus genome. *Biochem Biophys Res Commun* 215, 744–749.

Tokita, H., Okamoto, H., Iizuka, H., Kishimoto, J., Tsuda, F., Lesmana, L. A., Miyakawa, Y. & Mayumi, M. (1996). Hepatitis C virus variants from Jakarta, Indonesia classifiable into novel genotypes in the second (2e and 2f), tenth (10a) and eleventh (11a) genetic groups. *J Gen Virol* 77, 293–301.

Young, K. C., Lindsay, K. L., Lee, K. J., Liu, W. C., He, J. W., Milstein, S. L. & Lai, M. M. (2003). Identification of a ribavirin-resistant NS5B mutation of hepatitis C virus during ribavirin monotherapy. *Hepatology* 38, 869–878.

Zhou, S., Liu, R., Baroudy, B. M., Malcolm, B. A. & Reyes, G. R. (2003). The effect of ribavirin and IMPDH inhibitors on hepatitis C virus subgenomic replicon RNA. *Virology* 310, 333–342.

Zhu, Q., Guo, J. T. & Seeger, C. (2003). Replication of hepatitis C virus subgenomes in nonhepatic epithelial and mouse hepatoma cells. *J Virol* 77, 9204–9210.

THE JOURNAL OF BIOLOGICAL CHEMISTRY
Vol. 280, No. 13, Issue of April 1, pp. 12430–12437, 2005
Printed in U.S.A.

Centrosomal P4.1-associated Protein Is a New Member of Transcriptional Coactivators for Nuclear Factor-κB*

Received for publication, September 10, 2004, and in revised form, January 13, 2005
Published, JBC Papers in Press, January 31, 2005, DOI 10.1074/jbc.M410420200

Michiyo Koyanagi‡, Makoto Hijikata, Koichi Watashi, Osamu Masui, and Kunitada Shimotohno§

From the Department of Viral Oncology, Institute for Virus Research, Kyoto University, Sakyo-ku, Kyoto 606-8507, Japan

Nuclear factor-κB (NF-κB) is a transcription factor important for various cellular events such as inflammation, immune response, proliferation, and apoptosis. In this study, we performed a yeast two-hybrid screening using the N-terminal domain of the p65 subunit (RelA) of NF-κB as bait and isolated centrosomal P4.1-associated protein (CPAP) as a candidate for a RelA-associating partner. Glutathione *S*-transferase pull-down assays and co-immunoprecipitation experiments followed by Western blotting also showed association of CPAP with RelA. When overexpressed, CPAP enhanced NF-κB-dependent transcription induced by tumor necrosis factor-α (TNFα). Reduction of the protein level of endogenous CPAP by RNA interference resulted in decreased activation of NF-κB by TNFα. After treatment with TNFα, a portion of CPAP was observed to accumulate in the nucleus, although CPAP was found primarily in the cytoplasm without any stimulation. Moreover, CPAP was observed in a complex recruited to the transcriptional promoter region containing the NF-κB-binding motif. One hybrid assay showed that CPAP has the potential to activate gene expression when tethered to the transcriptional promoter. These data suggest that CPAP functions as a coactivator of NF-κB-mediated transcription. Since a physiological interaction between CPAP and the coactivator p300/CREB-binding protein was also observed and synergistic activation of NF-κB-mediated transcription was achieved by these proteins, CPAP-dependent transcriptional activation is likely to include p300/CREB-binding protein.

Nuclear factor-κB (NF-κB)[1] is a Rel transcription factor that regulates the expression of a wide variety of genes involved in cellular events such as inflammation, immune response, proliferation, and apoptosis (1–3). Rel family members form hetero- and homodimers that possess distinct specificities and functions. In mammals, five Rel family members have been identified: c-Rel, RelA/p65, RelB, NF-κB1 (p50/p105), and NF-κB2 (p52/p100). In the canonical NF-κB signaling pathway, the prototypical NF-κB complex composed of p50 and RelA subunits is sequestered in the cytoplasm through its assembly with a family of NF-κB inhibitors (IκB) at steady state. When cells are stimulated by signals such as tumor necrosis factor-α (TNFα) and interleukin-1, IκB is phosphorylated by the IκB kinase complex, marking it for ubiquitination and subsequent degradation. The liberated NF-κB heterodimer rapidly translocates into the nucleus and activates target genes by binding directly to κB regulatory elements present in the target loci.

Although these cytoplasmic signaling events are understood in detail, the subsequent nuclear events that regulate the strength and duration of NF-κB-mediated transcriptional activation remain poorly defined (4). RelA contains a transactivation domain (TAD) in its C-terminal region that is known to be responsible for transcriptional activation. TAD has so far been reported to interact with various transacting and basal transcription factors that recruit RNA polymerase II, including TATA-binding protein, transcription factor IIB, $TAF_{II}105$ (TATA-binding protein-associated factor II105), and TLS (translocated in liposarcoma) (5–8). In addition, general coactivators such as cAMP response element-binding protein (CREB)-binding protein (p300/CBP) (9, 10), p300/CBP-associated factor, and ACTR (coactivator for nuclear hormone receptors) are recruited to the NF-κB transcriptional complex and enhance NF-κB-mediated transcriptional activation (11, 12).

The N-terminal domain of RelA is also known to play important roles in the regulation of NF-κB-mediated transcriptional activation. For example, stimulus-coupled phosphorylation of RelA is known to change its transcriptional activity (4, 10, 13–16), and two of the four serine phosphoacceptor sites present in RelA are in the N-terminal domain. In addition, association with p300/CBP has been reported to occur not only via TAD, but also through the N-terminal domain of RelA. RelA phosphorylation at Ser^{276} by the catalytic subunit of cAMP-dependent protein kinase (14) or mitogen- and stress-activated protein kinase-1 (15) or at Ser^{311} by protein kinase Cζ (16) was shown to enhance the binding of p300/CBP to RelA. Moreover, p300/CBP has also been reported to acetylate RelA at three sites in the N-terminal domain: Lys^{218}, Lys^{221}, and Lys^{310}. Acetylation is thought to regulate the transcriptional activity of RelA by increasing its DNA-binding affinity for the κB enhancer or by preventing its association with IκBα (4, 17–20). Finally, BRCA1 also associates with the N-terminal domain of

* This work was supported in part by grants-in-aid for cancer research and for the second-term comprehensive 10-year strategy for cancer control from the Ministry of Health, Labor, and Welfare of Japan, by grants-in-aid for scientific research from the Ministry of Education, Culture, Sports, Science, and Technology of Japan, by grants-in-aid for research for the future from the Japanese Society for the Promotion of Science, and by the Program for Promotion of Fundamental Studies in Health Science of the Organization for Pharmaceutical Safety and Research of Japan. The costs of publication of this article were defrayed in part by the payment of page charges. This article must therefore be hereby marked "*advertisement*" in accordance with 18 U.S.C. Section 1734 solely to indicate this fact.

‡ Supported by the 21st Century Center of Excellence Program of the Ministry of Education, Culture, Sports, Science, and Technology of Japan to the Graduate School of Biostudies and the Institute for Virus Research, Kyoto University.

§ To whom correspondence should be addressed. Tel.: 81-75-751-4000; Fax: 81-75-751-3998; E-mail: kshimoto@virus.kyoto-u.ac.jp.

[1] The abbreviations used are: NF-κB, nuclear factor-κB; TNFα, tumor necrosis factor-α; TAD, transactivation domain; CREB, cAMP response element-binding protein; CBP, cAMP response element-binding protein-binding protein; CPAP, centrosomal P4.1-associated protein; STAT, signal transducer and activator of transcription; GST, glutathione *S*-transferase; siRNA, small interfering RNA; DBD, DNA-binding domain; SRC-1, steroid receptor coactivator-1; C/H, cysteine/histidine-rich.

RelA as well as CBP and functions as a scaffolding protein by tethering together the RelA-CBP-BRCA1 complex, thereby supporting the transacting function of CBP (21).

Thus, not only TAD, but also the N-terminal region of RelA appears to contribute to NF-κB target gene induction. However, little is known about the factors that interact with the N-terminal region. Here, we sought to clarify the mechanism of NF-κB-dependent transcriptional activation by identifying factors that interact with the N-terminal region of RelA. In a yeast two-hybrid screen using the N terminus of RelA as bait, we identified a novel RelA-interacting factor, centrosomal P4.1-associated protein (CPAP). CPAP was previously identified by virtue of its interaction with the cytoskeletal protein 4.1R-135 (22). Although CPAP appears to be a component of the centrosomal complex, the majority of CPAP is found in soluble fractions, mainly in the cytoplasm and a small portion in the nucleus (22, 23). In addition, it was previously reported that CPAP interacts with STAT5 and enhances STAT5-mediated transcription (23), although the mechanism by which this occurs remains unclear. In this study, we show evidence suggesting that CPAP is a novel coactivator of NF-κB that binds to the N-terminal region of RelA, possibly activating transcription through CBP.

EXPERIMENTAL PROCEDURES

Plasmid Construction—pEFr-FLAG-CPAP was a kind gift from Dr. J. E. Visvader (Walter and Eliza Hall Institute of Medical Research, Melbourne, Australia) (23). The cDNA fragment consisting of the entire open reading frame of CPAP was generated by PCR using a human spleen cDNA library (Clontech, Palo Alto, CA) as the template and primers 5′-CGCGGATCCATGTTCCTGATGCCAACCTC-3′ and 5′-TTTTCCTTTTGCGGCC GCATCGTCACAGCTCCGTGTCC-3′. The fragment was inserted into the BamHI-NotI sites of the pcDNA3-Myc vector (24) to construct pcDNA3-Myc-CPAP and blunt-end cloned into the pCMV-FLAG vector (24) to generate pCMV-CPAP. The series of plasmids encoding deletion mutants of CPAP, pcDNA3-Myc-CPAP-(1–1149), pcDNA3-Myc-CPAP-(1150–1338), and pcDNA3-Myc-CPAP-(967–1338), was constructed by inserting fragments generated by PCR using appropriate synthetic oligonucleotides as primers and pcDNA3-Myc-CPAP as the template. pcDNA3-HA-RelA (where HA is hemagglutinin), pcDNA3-HA-RelA-(1–427), pcDNA3-HA-RelA-(428–551), pcDNA3-HA-RelA-(1–312), pcDNA3-HA-RelA-(313–427), and pcDNA3-HA-RelA-(201–427) were generated in a similar manner using pcDNA3-RelA (25) as the template.

pGEX-2TK-RelA was created by inserting the RelA BamHI-MfeI fragment into the BamHI-EcoRI sites of the pGEX-2TK vector (Clontech). pFastBac1-RelA was constructed by inserting the glutathione *S*-transferase (GST)-RelA fragment of pGEX-2TK-RelA into the BamHI-XbaI sites of the pFastBac1 vector (Invitrogen). pGEX-CPAP-C was created by inserting the EcoRI-NotI fragment of pcDNA3-Myc-CPAP-(967–1338) into the EcoRI-NotI sites of the pGEX-6P-1 vector (Clontech).

pM-CPAP was generated by inserting the BamHI-XbaI fragment, which was PCR-amplified from pcDNA3-Myc-CPAP using primers 5′-CGCGGATCCCAATGTTCCTGATGCCAACCTC-3′ and 5′-GCTCTAGAATCGTCACAGCTCCGTGTCC-3′, into the BamHI-XbaI sites of the pM vector (Clontech). pM-CPAP-(967–1338) was obtained by inserting the EcoRI-XbaI fragment of pcDNA3-Myc-CPAP-(967–1338) into the EcoRI-XbaI sites of the pM vector.

pCMV-CBP was a kind gift from Dr. I. Talianidis (Institute of Molecular Biology and Biotechnology, Crete, Greece) (26). The expression plasmids for a series of CBP deletion mutants (CBP1–CBP5) were kindly provided by Dr. A. Fukamizu (Center for Tsukuba Advanced Research Alliance, Tsukuba, Japan) (27). The reporter plasmids pNF-κB-luc and pFR-luc were obtained from Stratagene. The construction of the reporter plasmid pNF-κB-mt-luc was described previously (28).

Yeast Two-hybrid Screening—The DNA fragment encoding amino acids 1–427 of RelA was subcloned into the pHybLex-Zeo vector (Invitrogen). This plasmid was used as a bait construct to screen a human leukemia cDNA library (Clontech) according to the manufacturer's instructions (Invitrogen). A total of 1.6×10^6 transformants were selected based on histidine prototrophy and β-galactosidase activity.

GST Pull-down Assay—GST and the GST-RelA fusion protein, encoded by pFastBac1 and pFastBac1-RelA, respectively, were produced in Sf9 cells using the Bac-to-Bac baculovirus expression system (Invitrogen). GST and the GST-CPAP-(967–1338) fusion protein, encoded by pGEX-6P-1 and pGEX-CPAP-(967–1338), respectively, were produced in BL21 cells (Amersham Biosciences) exposed to 0.1 mM isopropyl β-D-thiogalactopyranoside. After affinity separation of the proteins from cell lysates using glutathione-Sepharose (Amersham Biosciences), proteins bound to the resin were mixed and incubated with *in vitro* transcription/translation products at 4 °C for 2 h. The *in vitro* transcription/translation product was prepared with the TNT T7 quick coupled transcription/translation system (Promega) using 0.25 μg of each expression plasmid in the presence of L-[^{35}S]methionine (Amersham Biosciences) according to the manufacturer's instructions. After being washed five times in binding buffer (50 mM Tris-HCl (pH 8.0), 150 mM NaCl, 1 mM EDTA, 0.5% Nonidet P-40, 1 mM dithiothreitol, and 1 mM phenylmethylsulfonyl fluoride), resin-bound radiolabeled proteins were fractionated by SDS-PAGE and detected by autoradiography.

Cell Culture and Transfection—293T and MCF-7 cells were cultured in Dulbecco's modified Eagle's medium (Nissui) supplemented with 10% fetal bovine serum and L-glutamine. Transfection of plasmids into cells was performed with FuGENE 6 transfection reagent (Roche) according to the manufacturer's recommendations.

Immunoprecipitation—Cells were lysed in immunoprecipitation buffer (50 mM Tris-HCl (pH 7.5), 150 mM NaCl, and 0.1% Nonidet P-40). After centrifugation, the supernatant was incubated with anti-FLAG antibody M2 (Sigma), anti-RelA antibody F-6 (Santa Cruz Biotechnology, Inc.), anti-c-Myc antibody 9E10 (Santa Cruz Biotechnology, Inc.), or normal mouse IgG (Zymed Laboratories Inc.) for at least 1 h. Immunocomplexes were recovered by adsorption to protein G-Sepharose (Amersham Biosciences). After being washed five times in immunoprecipitation buffer, the immunoprecipitates were analyzed by immunoblotting.

Immunoblot Analysis—Immunoblot analysis was performed essentially as described previously (29). The antibodies used in these experiments were specific for FLAG, RelA (antibody F-6), and α-tubulin (antibody-1, Calbiochem). The rabbit antiserum against CPAP was kindly provided from Dr. T. K. Tang (Institute of Biomedical Sciences, Taipei, Taiwan, Republic of China) (22).

Reporter Assay—Cell extracts were prepared in reporter lysis buffer (Promega) 48 h after transfection. After removal of cell debris, the luciferase activity in the extracts was measured with a luciferase assay kit (Promega) and a Berthold Lumat LB 9507 luminometer according to the manufacturers' instructions.

RNA Interference Technique—A 21-nucleotide small interfering RNA (siRNA) duplex (5′-AAUGGAAUGCACGUGACGAUG-3′) containing 3′-dTdT overhanging sequences was synthesized (Qiagen Inc.). siRNA transfection was performed using Oligofectamine reagent (Invitrogen) according to the manufacturer's instructions.

RNA Isolation and Reverse Transcription-PCR—Total RNA was isolated from cultured cells using Sepasol RNA I Super (Nacalai Tesque, Kyoto, Japan) according to the manufacturer's instructions. The relative expression of each mRNA was evaluated by semiquantitative reverse transcription-PCR using a One-Step RNA PCR kit (Takara). Glyceraldehyde-3-phosphate dehydrogenase mRNA was used as an internal control. The primers used were as follows: CPAP, 5′-AAAGGGACCACAGGTAGCGG-3′ and 5′-TGAATTCACTCGCACGATCTGGGATG; interferon-β, 5′-CACGACAGCTCTTTCCATGA-3′ and 5′-AGCCAGTGCTCGATGAATCT-3′; and TNF receptor-associated factor-1, 5′-GCCCCTGATGAGAATGAGTT-3′ and 5′-CTCATGCTCTTGCACAGACT-3′.

Indirect Immunofluorescence Analysis—Indirect immunofluorescence analysis was performed as described previously (29). Cells were permeabilized with 0.05% Triton X-100 after fixation and treated with anti-RelA primary antibody F-6 or rabbit antiserum against CPAP (22). Secondary antibodies conjugated to Alexa 488 and Alexa 568 (Molecular Probes, Inc.) were used to visualize primary antibody distribution. Nuclei were stained with 4′,6-diamidino-2-phenylindole (Sigma).

DNA-Protein Complex Immunoprecipitation Assay—293T cells treated with 10 nM TNFα were transfected with plasmids. After cross-linking with 1% formaldehyde for 15 min, cells were lysed; sonicated; and subjected to immunoprecipitation using anti-FLAG or anti-RelA antibody or normal mouse IgG. Recovered immunocomplexes were incubated at 65 °C for 16 h and then digested with proteinase K for 2 h. DNA was extracted from the immunocomplexes with phenol and precipitated with ethanol. The primers used for detection of recovered DNA were 5′-ACCGAAACGCGCGAGGCAGGATCAGCCATA-3′ and 5′-GCTCTCCAGCGGTTCCATC-3′ for pNF-κB-luc and 5′-CTAGCAAAATAGGCTGTCCC-3′ and 5′-CTTTATGTTTTTGGCGTATTCCA-3′ for pNF-κB-mt-luc.

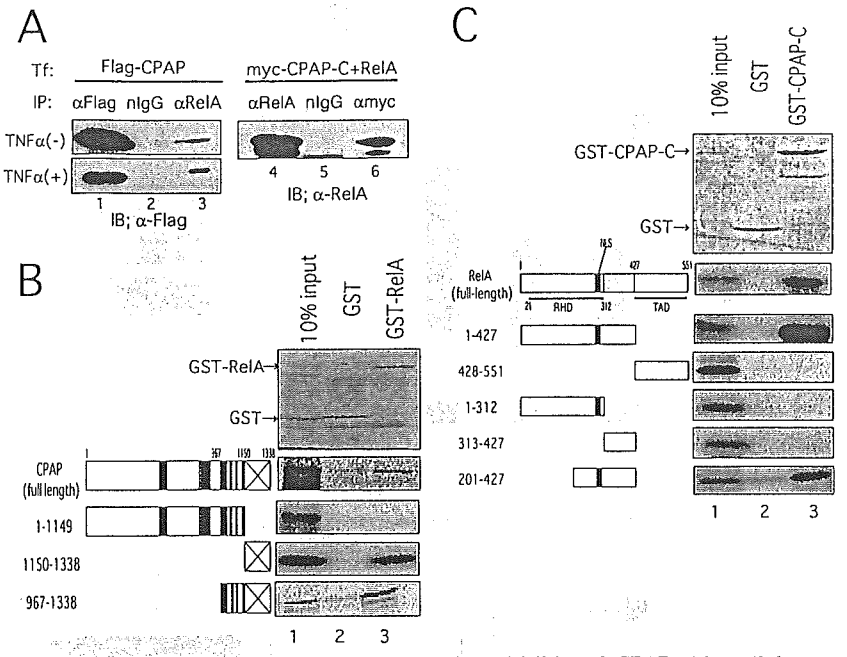

FIG. 1. **Interaction between RelA and CPAP.** *A*, interaction between RelA and full-length CPAP without (*left upper panel*) and with (*left lower panel*) TNFα stimulation or the C-terminal domain of CPAP from amino acids 967 to 1338 (CPAP-C) (*right panel*). Lysates from 293T cells transfected with 10 μg of pEFr-FLAG-CPAP or 8 μg of pcDNA3-Myc-CPAP-C and 2 μg of pcDNA3-RelA were used for the immunoprecipitation analysis. *Tf* and *IP* denote proteins produced from the transfected plasmids and antibodies used in the immunoprecipitation experiments, respectively. *αFLAG*, *nIgG*, *αRelA*, and *αmyc* indicate anti-FLAG antibody, normal mouse IgG, anti-RelA antibody, and anti-Myc antibody, respectively. FLAG-tagged CPAP and RelA in the immunoprecipitates were detected by immunoblotting (*IB*) using anti-FLAG and anti-RelA antibodies, respectively. *B*, mapping of the region of CPAP responsible for interaction with RelA by deletion analysis. The ^{35}S-labeled *in vitro* transcription/translation product of full-length CPAP or its deletion mutants was incubated with GST (*lane 2*) or GST-RelA (*lane 3*) immobilized on glutathione-Sepharose. The proteins bound to the resin were eluted, resolved by SDS-PAGE, and visualized by autoradiography (*lower panel*). *10% input* indicates 0.1 volume of the ^{35}S-labeled product used in the pull-down assay (*lane 1*). The Coomassie Brilliant Blue staining pattern of proteins pulled down from the reaction mixture containing full-length CPAP is shown as an example (*upper panel*). Bands representing GST and GST-RelA are indicated by *arrows*. A schematic representation of the structures of CPAP and its deletion mutants is shown on the left. CPAP contains a leucine zipper motif (*gray boxes*), a series of nonamer glycine repeats (G-box region; *crossed boxes*), three putative nuclear localization signals (*dashed boxes*), and two potential nuclear export signals (*black boxes*). The *numbers* indicate the amino acids demarcating fragments of the CPAP protein used. *C*, mapping of the RelA region that interacts with CPAP by deletion analysis. The ^{35}S-labeled product of full-length RelA or its truncated mutants was incubated with GST (*lane 2*) or GST-CPAP-C (*lane 3*). The Coomassie Brilliant Blue staining pattern of proteins pulled down from the reaction mixture with full-length RelA is shown as an example (*upper panel*). The bands representing GST and GST-CPAP-C are indicated by *arrows*. A schematic representation of RelA and its mutants is shown on the left. RelA contains a Rel homology domain (*RHD*), a nuclear localization signal (*NLS*), and a TAD.

RESULTS

Identification of CPAP as a Factor That Interacts with RelA—To identify cellular factors that interact with the N-terminal region of RelA, a yeast two-hybrid screen was performed using a human leukemia cDNA library as bait and the N-terminal 427-amino acid region of RelA as prey. From 1.6×10^6 L40 yeast transformants, 64 clones were obtained that appeared to interact with RelA. Among them, three independent clones were revealed to encode portions of CPAP.

To confirm the interaction of CPAP with RelA, we performed an immunoprecipitation assay using 293T cells exogenously producing FLAG-tagged CPAP. FLAG-tagged CPAP was detected in cell lysates in the immunocomplex formed with anti-RelA antibody (Fig. 1*A*, *left panels*, *lane 3*), but not with normal IgG (*lane 2*). The interaction between FLAG-tagged CPAP and endogenous RelA was seen without considerable alteration both before and after treatment with TNFα (Fig. 1*A*, *upper* and *lower left panels*, respectively). This seemed to imply that TNFα-induced phosphorylation of RelA is not essential for the interaction with CPAP. Actually, we found that FLAG-tagged CPAP was co-immunoprecipitated with a RelA mutant in which one of the TNFα-induced phosphorylation target sites (Ser^{276}) was replaced with alanine (data not shown). This may support the above idea. This interaction was also seen in a GST pull-down assay. Under conditions in which *in vitro* translated CPAP was not pulled down with GST-bound Sepharose beads (Fig. 1*B*, *lane 2*), we found it in a pellet with recombinant GST-RelA-bound Sepharose beads (*lane 3*). These results suggest that CPAP interacts specifically with RelA. In addition, to examine the region of CPAP responsible for interaction with RelA, we performed a GST pull-down assay as described above using several deletion mutants of CPAP. The *in vitro* synthesized fragments of CPAP spanning amino acids 1150–1338 and 967–1338, but not amino acids 1–1149, were co-purified with GST-RelA (Fig. 1*B*). This indicates that the region of CPAP responsible for interaction with RelA resides within amino acids 1150–1338, including a series of 21 nonamer repeats (G-box region). This result was also obtained with the immunoprecipitation assay. In the lysates of 293T cells producing RelA and Myc-tagged CPAP-C (C-terminal amino acids 967–1338 of CPAP), exogenous RelA was efficiently detected in immunocomplexes formed with anti-Myc antibody (Fig. 1*A*, *right panel*, *lane 6*), but not with normal mouse IgG (*lane 5*). The region of RelA that interacts with CPAP was similarly assessed. The *in vitro* synthesized fragments of RelA spanning amino acids 1–427 and 201–427, but not amino acids 428–551, 1–312, or 313–427, were co-purified with GST-CPAP-C (Fig. 1*C*). These results indicate that the central region of RelA is necessary and sufficient for interaction with CPAP.

CPAP Augments NF-κB-dependent Gene Expression—Because CPAP has been reported to activate STAT5-mediated transcription (23), we examined the effect of this protein on RelA-mediated transcription using a reporter assay. When CPAP was ectopically expressed, NF-κB-responsive reporter gene expres-

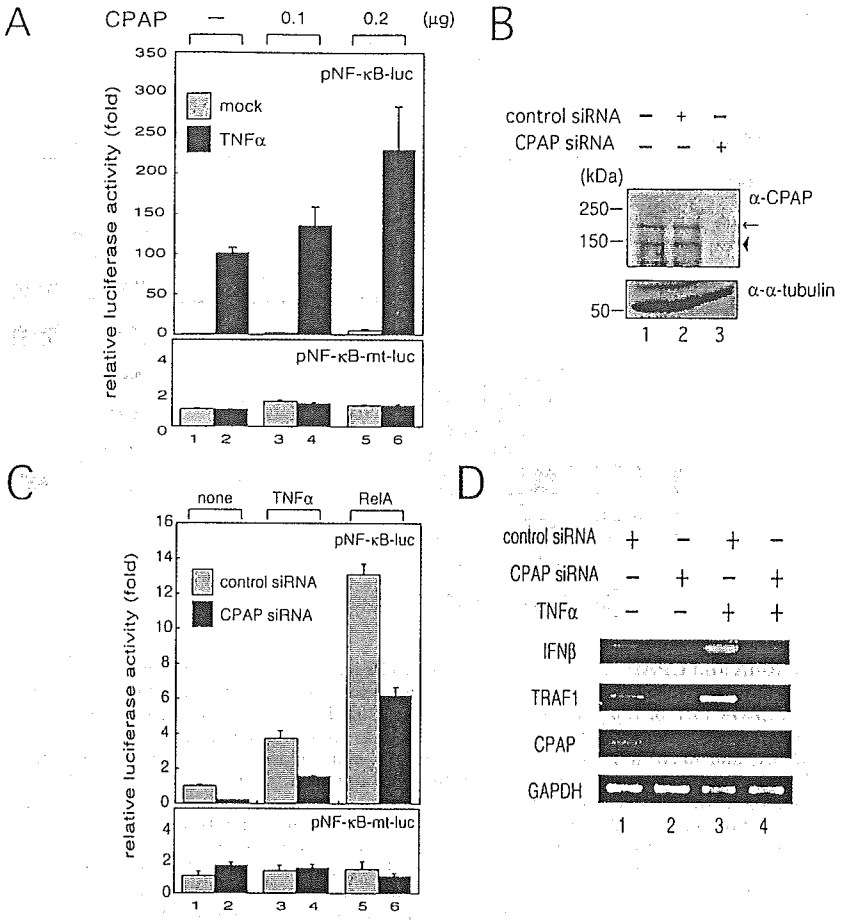

FIG. 2. **CPAP increases NF-κB-induced gene expression.** *A*, enhancement of NF-κB-dependent reporter gene expression by ectopic expression of CPAP. 293T cells were transfected with 25 ng of pNF-κB-luc (containing wild-type NF-κB-binding sites upstream of the luciferase gene; *upper panel*) or pNF-κB-mt-luc (containing mutated NF-κB-binding sites; *lower panel*) together with the indicated amounts of pCMV-FLAG-CPAP. After 42 h of transfection, cells were mock-treated (*bars 1*, *3*, and *5*) or treated with 10 ng/ml TNFα (*bars 2*, *4*, and *6*) and harvested after an additional incubation for 6 h. Values represent the relative luciferase activity expressed as the mean ± S.E. of three independent transfections. *B*, suppression of endogenous CPAP production by siRNA. The 21-nucleotide RNA duplex (siRNA) directed against the CPAP sequence was transfected into MCF-7 cells (*lane 1*). The levels of CPAP protein were evaluated by immunoblotting 48 h post-transfection. As a negative control, total cell extracts from MCF-7 cells with no siRNA treatment (*lane 1*) and with treatment with control siRNA (*lane 2*) were used. The relative protein levels of CPAP (*upper panel*) and α-tubulin as a positive control (*lower panel*) are shown. Molecular mass markers are shown on the left. The *arrow* indicates intact CPAP protein. The *arrowhead* shows the putative degraded form of CPAP. *C*, effects of CPAP siRNA on NF-κB-dependent reporter gene expression. MCF-7 cells were transfected with control siRNA (*gray bars*) or CPAP siRNA (*black bars*). At 24 h post-transfection, 25 ng of pNF-κB-luc, 25 ng of pRL-TK-luc, and 200 ng of either pKS$^+$-CMV (*bars 1–4*) or pcDNA3-RelA (*bars 5* and *6*) were transfected into cells (*upper panel*). The same experiment using pNF-κB-mt-luc instead of pNF-κB-luc was also carried out (*lower panel*). An additional 18 h later, cells were treated with (*bars 3* and *4*) or without (*bars 1*, *2*, *5*, and *6*) 10 ng/ml TNFα for 6 h. Values represent the luciferase activity expressed as the mean ± S.E. of three independent transfections. *D*, effects of CPAP siRNA on endogenous gene expression induced by TNFα. MCF-7 cells were transfected with control (*lanes 1* and *3*) or CPAP siRNA (*lane 2* and *4*). The cells were treated for 6 h with 10 ng/ml TNFα (*lanes 3* and *4*). Semiquantitative reverse transcription-PCR was performed to estimate the amounts of interferon-β (*IFNβ*), TNF receptor-associated factor-1 (*TRAF1*), CPAP, and glyceraldehyde-3-phosphate dehydrogenase (*GAPDH*) mRNAs.

sion was enhanced by up to 2–3-fold in a dose-dependent manner (Fig. 2*A*, *upper panel*). In contrast, reporter activity from the plasmid containing mutated NF-κB-binding sites in the promoter region was not affected by ectopically expressed CPAP (Fig. 2*A*, *lower panel*). These data suggest that CPAP can specifically up-regulate NF-κB-mediated transcription.

To investigate the contribution of endogenous CPAP to transcriptional activation, we examined the effect of CPAP siRNA, which was designed to specifically knock down the expression of CPAP, on NF-κB-dependent transcriptional activation in MCF-7 breast cancer-derived cells. We confirmed that endogenous CPAP protein levels were significantly reduced by transfection with CPAP siRNA, whereas the levels of other cellular proteins such as α-tubulin were not changed (Fig. 2*B*). The level of NF-κB-mediated transcription induced by either TNFα or RelA in CPAP siRNA-treated cells was decreased to <50% of that in cells transfected with control siRNA (Fig. 2*C*, *upper panel*). In contrast, reporter activity from the plasmid containing mutated NF-κB-binding sites was not affected by knocking down CPAP (Fig. 2*C*, *lower panel*). These findings indicate that endogenous CPAP is required for full activation of NF-κB-dependent reporter gene expression.

Next, we examined whether CPAP affects expression of endogenous target genes. After treatment with TNFα, total RNA was isolated from MCF-7 cells transfected with either control or CPAP siRNA and analyzed by reverse transcription-PCR to detect the mRNA levels of interferon-β and TNF receptor-associated factor-1, which are known to be induced by NF-κB. As shown in Fig. 2*D*, transfection with CPAP siRNA, but not control siRNA, down-regulated TNFα-induced expression of interferon-β and TNF receptor-associated factor-1 mRNAs. These results indicate that CPAP plays an important role in NF-κB-mediated transcriptional activation in cells.

Translocation of CPAP into the Nucleus upon TNFα Treatment—RelA is translocated from the cytoplasm into the nucleus upon stimulation by specific cytokines. To determine

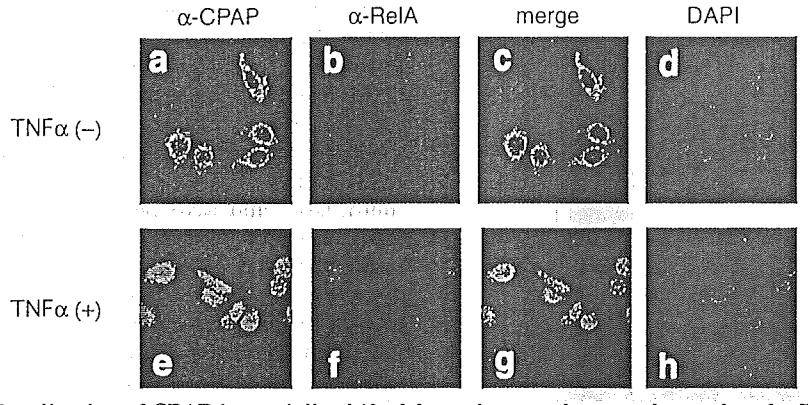

FIG. 3. **The subcellular localization of CPAP is partially shifted from the cytoplasm to the nucleus by TNFα stimulation.** Indirect immunofluorescence analysis was performed on MCF-7 cells treated with (*lower panels*) or without (*upper panels*) TNFα for 20 min. The antibodies used in this experiment were anti-CPAP (*α-CPAP*; *a* and *e*, *green*) and anti-RelA (*α-RelA*; *b* and *f*, *red*). Merged images of *green* and *red* signals are shown (*c* and *g*). 4′,6-Diamidino-2-phenylindole (*DAPI*) was used to visualize nuclear staining (*d* and *h*).

whether the localization of CPAP is similarly altered by activation of the NF-κB pathway, we examined the subcellular localization of CPAP in MCF-7 cells by indirect immunofluorescence analysis with or without TNFα treatment. As reported previously (23), CPAP was found to localize primarily in the cytoplasm, although some protein was also detectable in the nucleus without stimulation (Fig. 3*a*). As CPAP was immunoprecipitated with RelA from the cytoplasmic fraction of such cells (data not shown), it seemed likely that a cytoplasmic complex is present before TNFα treatment. However, following TNFα treatment for 20 min, a portion of CPAP was observed to accumulate in the nucleus (Fig. 3*e*), similar to RelA (*b* and *f*). These results suggest that at least a portion of cytoplasmic CPAP enters the nucleus in a TNFα-dependent manner.

Recruitment of CPAP to the NF-κB-binding Motif—The increase in NF-κB-dependent transcriptional activation by CPAP, the nuclear accumulation of CPAP in response to TNFα stimulation, and the physical interaction of CPAP with RelA all suggested the possibility that CPAP, together with RelA, is recruited to the transcriptional promoters of NF-κB target genes. To examine this possibility, we performed a DNA-protein complex immunoprecipitation assay. As shown in Fig. 4 (*upper panel*, *lanes 1–3*), a DNA fragment containing an NF-κB-binding motif was detected by PCR in complexes specifically immunoprecipitated by either anti-FLAG or RelA antibodies from lysates of 293T cells transfected with pNF-κB-luc, FLAG-tagged CPAP, and RelA expression plasmids. In contrast, no DNA fragment was amplified from cells transfected with pNF-κB-mt-luc instead of pNF-κB-luc (Fig. 4, *lower panel*, *lanes 2* and *3*). These data suggest that CPAP is recruited to the transcriptional promoter region containing an NF-κB-binding motif via association with RelA.

CPAP Can Activate Gene Expression When Tethered to a Transcriptional Promoter—We showed above that CPAP interacted with RelA, up-regulated NF-κB-mediated transcription, and formed part of the complex binding to a transcriptional promoter containing NF-κB-binding motifs. These data suggest that CPAP acts as a transcriptional coactivator of NF-κB. We examined this possibility using a one-hybrid assay system with fusion proteins consisting of the Gal4 DNA-binding domain (DBD) and full-length CPAP or its C-terminal region in mammalian cells. As demonstrated in Fig. 5 (*second bar*), Gal4 DBD-fused CPAP up-regulated luciferase expression from pFR-luc, a reporter plasmid containing a Gal4-responsive transcriptional promoter. In contrast, CPAP by itself had no effect on the same promoter (Fig. 5, *third bar*). No difference in luciferase levels was observed among the exogenous Gal4 DBD-containing constructs (data not shown). This suggests that

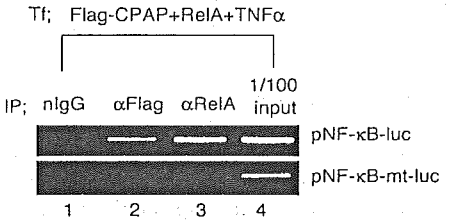

FIG. 4. **Recruitment of CPAP to a promoter containing an NF-κB-binding motif.** 293T cells cotransfected with expression plasmids for RelA and FLAG-CPAP and pNF-κB-luc (*upper panel*) or pNF-κB-mt-luc (*lower panel*) were harvested after treatment with TNFα for 20 min. After formaldehyde fixation, the cross-linked DNA-protein complexes were immunoprecipitated with anti-RelA antibody (*αRelA*; *lane 3*), anti-FLAG antibody (*αFLAG*; *lane 2*). or normal mouse IgG (*nIgG*; *lane 1*). 1% input of total cell lysate was used as positive control (*lane 4*). The DNA extracted from each immunoprecipitate was used as the template for PCR to detect the DNA fragment containing NF-κB-binding motifs as described under "Experimental Procedures." *Tf* and *IP* denote proteins produced from the transfected plasmids and antibodies used in the immunoprecipitation experiments, respectively.

CPAP has a transactivation capacity when tethered to the transcriptional promoter. This activity is likely to be located in the C-terminal part of CPAP because this region showed higher reporter activation compared with full-length CPAP (Fig. 5, *fourth* and *second bars*, respectively). Together with our results above, these data suggest that CPAP acts as a transcriptional coactivator in the NF-κB transcriptional complex.

Interaction between CPAP and CBP—To obtain insights into the mechanism of CPAP-dependent transcriptional activation, we assessed whether CPAP can recruit known coactivators to the transcriptional promoter. First, we examined the physical association of CPAP with CBP, p300, steroid receptor coactivator-1 (SRC-1), and transcription intermediary factor-2 using a GST pull-down assay. *In vitro* synthesized CBP or p300, but not SRC-1 or transcription intermediary factor-2, was co-purified with GST-CPAP-C, whereas none could be pulled down by GST itself (Fig. 6*A*) (data not shown), suggesting that CPAP interacts with CBP and p300. To narrow down the region of CBP required for interaction with CPAP, deletion analysis was carried out using five CBP fragments, CBP1–CBP5 (27), which were produced and metabolically labeled in cells. Only CBP4, which contains the C/H3 domain, could be co-purified with GST-CPAP-C (Fig. 6*B*), suggesting that CPAP associates with CBP through this region of CBP.

Next, we performed a reporter assay to examine the effect of CPAP on NF-κB-mediated transcription. As shown in Fig. 6*C*, overexpression of either CBP or CPAP in cells enhanced TNFα-induced NF-κB-dependent transcription by ~2–3-fold

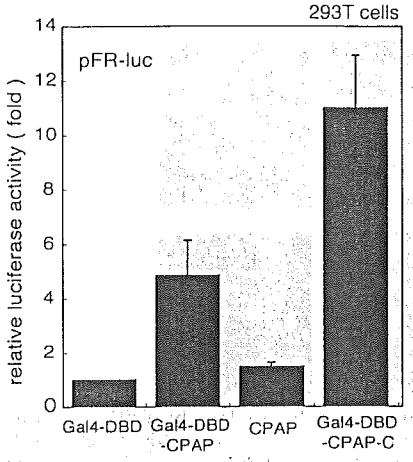

FIG. 5. **CPAP supports transcriptional activation when tethered to the promoter.** 293T cells were transfected with 50 ng of pFR-luc together with 0.3 μg of pM, pM-CPAP, pCMV-FLAG-CPAP, or pM-CPAP-C. After 48 h of transfection, cells were harvested and subjected to a luciferase assay. Values represent the relative luciferase activity expressed as the mean ± S.E. of three independent transfections.

compared with untransfected cells. When both CBP and CPAP were overexpressed in cells, reporter gene expression was synergistically elevated to levels 10-fold higher than in untransfected cells. These results suggest that CPAP contributes to NF-κB-dependent transcriptional activation at least partly by binding CBP and recruiting it to the cellular transcriptional machinery.

DISCUSSION

We identified CPAP as a molecule that associates with RelA and contributes to RelA-mediated transcriptional activation. Although CPAP was previously identified as a centrosomal protein (22), its function was not clear. Recently, however, CPAP was reported to interact with STAT5 to enhance STAT5-mediated transcription (23). However, the mechanism of CPAP-mediated transcriptional activation remained unclear. In this study, we have presented data showing that CPAP is a component of the NF-κB transcriptional activation complex and can activate transcription when tethered to a promoter. Moreover, we found that the transcriptional coactivator CBP contributes at least in part to transcriptional activation by association with CPAP.

Because CPAP fused with Gal4 DBD, but not CPAP itself, could induce reporter gene expression under the control of a promoter with Gal4-responsive elements (Fig. 5), CPAP is likely to activate transcription when presented to the transcriptional machinery. We also observed that CPAP exists in a DNA-protein complex including RelA and an NF-κB-responsive element, suggesting that CPAP binds to the promoter of NF-κB target genes in association with RelA to activate transcription. Enhancement of STAT5-mediated transcription by CPAP could be explained by a similar mechanism because CPAP was shown to interact with STAT5a/b as well as RelA. These data suggest that CPAP is a transcriptional coactivator.

The C-terminal 372 amino acids of CPAP exhibited transcriptional activation capability when fused with Gal4 DBD, suggesting that this region is responsible for transcriptional activation. This region associates with CBP, indicating that CBP may be involved in the transcriptional activation potential of CPAP. CBP is known to activate transcription by two mechanisms. CBP functions as a molecular bridge between the basal transcriptional machinery and transcription factors recruited to specific enhancer elements. In addition, the histone acetyltransferase activity of CBP plays an essential role in opening up chromatin structure to allow for efficient transcriptional activity (30, 31). Previous work also showed that p300/CBP binds to RelA and supports NF-κB-mediated transcriptional activation (9, 10). Here, we have shown that CPAP can associate with p300/CBP as well as RelA, indicating that these three proteins may form a complex. The breast cancer-related BRCA1 has been proposed to function as a scaffolding protein that tethers several factors, including RelA, CBP, and RNA polymerase II, to transcriptional promoter elements (21). By analogy with BRCA1, it seems likely that CPAP supports the transactivating effects of CBP by acting as a scaffolding protein that stabilizes CBP within the NF-κB transcriptional complex. We have shown that the C-terminal domain of CPAP interacts with the C-terminal region of p300/CBP containing the C/H3 and glutamine-rich domains. It was previously reported that the C-terminal TAD of RelA interacts mainly with the N-terminal region of p300/CBP containing the C/H1 and KIX domains (9, 10), which is distinct from the region that interacts with CPAP. These results may provide a structural framework for the formation of a complex including these three factors. However, the interactions are likely rather more complex because the C-terminal region of CPAP has also been identified as a RelA-interacting region. Furthermore, we already found that CPAP forms multimer (data not shown). Therefore, stoichiometric analysis will be required to unveil the functional structure of this mysterious complex as well as to better understand the molecular mechanism of CPAP-dependent transcriptional activation.

It is well known that some CBP-associated transcriptional coactivators such as p300/CBP-associated factor, SRC-1, and ACTR have histone acetyltransferase activity (32–34). Some members of the p300/CBP-associated factor-related family with strong histone acetyltransferase activity, such as GCN5, have a conserved amino acid sequence called motif A (35), which is considered to be a characteristic structural feature of histone acetyltransferase. However, we have not found any amino acid sequences similar to motif A in CPAP. On the other hand, it has been reported that the histone acetyltransferase domains of SRC-1 and ACTR members of the SRC family with relatively low histone acetyltransferase activity share regions of high glutamine content (33, 34). Because CPAP has multiple glycine or glutamine repeats in the C-terminal region shown to have transcriptional activation capacity, it is possible that CPAP possesses histone acetyltransferase activity in the C-terminal region. To determine whether this is in fact the case, biochemical analysis using purified CPAP is required in the future.

Besides functioning as a transcriptional coactivator, CPAP might also affect interactions between RelA and molecules that inhibit NF-κB-mediated transcription, such as IκB, histone deacetylase-1 (13), and RelA-associated inhibitor (36). Histone deacetylase-1 has been reported to interact directly with the N-terminal region of RelA to exert its corepressor function (13). RelA-associated inhibitor, which binds to the central region of RelA, has also been reported to inhibit RelA-mediated transcriptional activation via an unknown mechanism (36). As we have already detected that IκBα was coprecipitated with a CPAP-RelA complex from the cell lysate (data not shown), it may be unlikely that the presence of IκBα precludes the association of RelA and CPAP. Further analysis of the complex including RelA and CPAP under physiological conditions should provide valuable insight into the regulatory mechanism of NF-κB-dependent transcriptional activation.

In addition, we found that the subcellular localization of CPAP was partially altered from the cytoplasm to the nucleus upon TNFα treatment. It was also previously reported that CPAP, which binds to STAT5, translocates from the cytoplasm

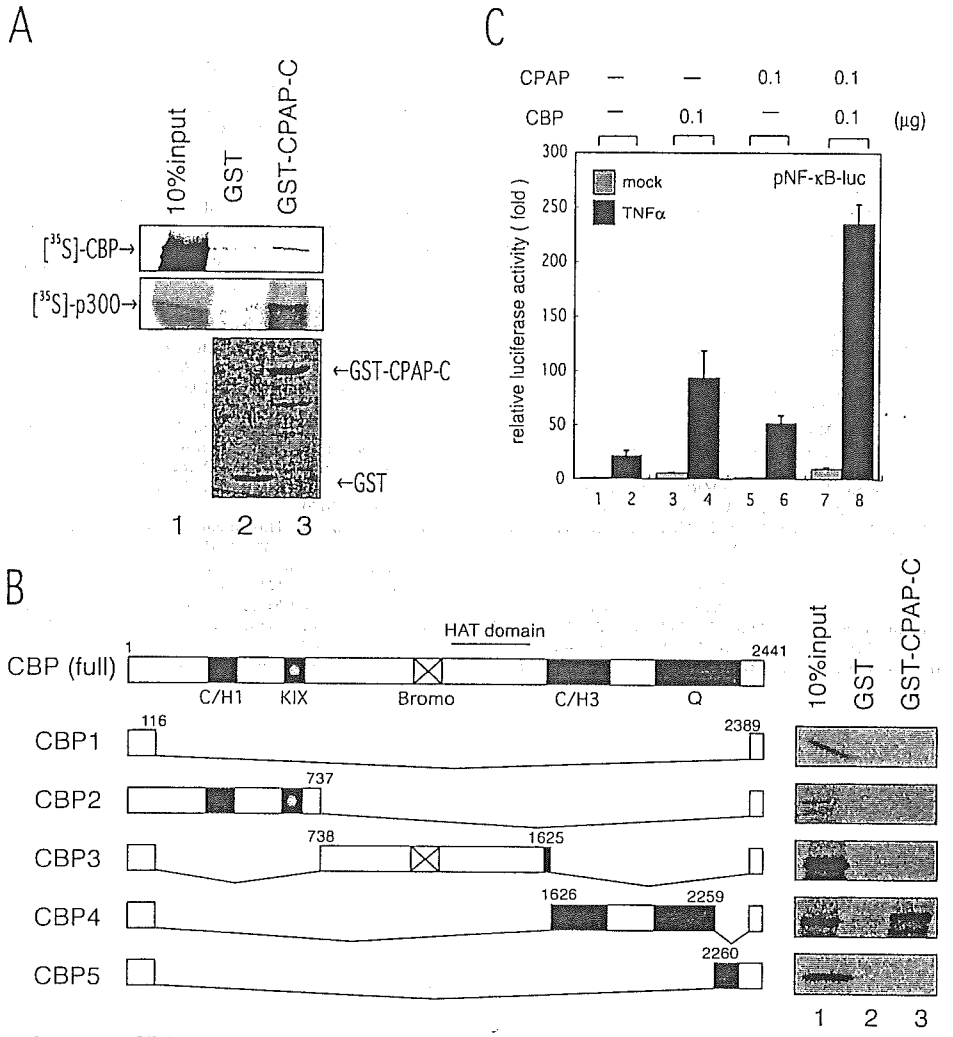

FIG. 6. **Association between CPAP and CBP.** *A*, results from a GST pull-down assay performed as described under "Experimental Procedures." ^{35}S-Labeled full-length CBP (*upper panel*) or p300 (*middle panel*) was incubated with recombinant GST (*lane 2*) or GST-CPAP-C (*lane 3*). *10%input* indicates 0.1 volume of the ^{35}S-labeled product used in the pull-down assay (*lane 1*). The Coomassie Brilliant Blue staining pattern of GST fusion proteins is shown (*lower panel*). *B*, mapping of the region of CBP that interacts with CPAP by deletion analysis. A schematic representation of the structures of CBP and its deletion mutants (CBP1–CBP5) is shown on the left. *Numbers* above the diagrams indicate the amino acid positions of CBP relative to the N terminus. C/H1 and C/H3 are the cysteine/histidine-rich regions, and KIX is the CREB-binding domain. *Bromo*, bromodomain; *Q*, glutamine-rich domain. The results of the GST pull-down assay using the C-terminal region of CPAP and a series of deletion mutants of CBP are shown on the right. ^{35}S-Labeled CBP1–CBP5 were incubated with recombinant GST (*lane 2*) or GST-CPAP-C (*lane 3*). *HAT*, histone acetyltransferase. *C*, synergistic enhancement of NF-κB-dependent reporter gene expression by CPAP and CBP. 293T cells were transfected with 25 ng of pNF-κB-luc together with the indicated amounts of pCMV-FLAG-CPAP (*CPAP*; *bars 5–8*) and/or pCMV-CBP (*CBP*; *bars 3, 4, 7,* and *8*). After 42 h of transfection, cells were treated with (*black bars 2, 4, 6,* and *8*) or without (*mock*; *gray bars 1, 3, 5,* and *7*) 10 ng/ml TNFα and harvested after an additional incubation for 6 h. Values represent the luciferase activity expressed as the mean ± S.E. of three independent transfections.

to the nucleus in response to prolactin-mediated activation of the JAK-STAT pathway and enhances STAT5-dependent transcription (23). As it has been reported that CPAP has three putative nuclear localization signals in its C-terminal region (23), it seems possible that CPAP is retained in the cytoplasm somehow in the steady state of cells, but released by particular stimuli. It has been revealed that ACTR, which is located mainly in the cytoplasm with a small portion in the nucleus in most cells, translocates from the cytoplasm to the nucleus upon TNFα activation and subsequent phosphorylation by IκB kinase-β (37). Further study on the molecular mechanism of stimulation-dependent nuclear translocation of CPAP may provide new knowledge regarding the fine regulation of gene expression by extracellular stimuli.

In this study, we have shown that CPAP can modulate RelA function in the nucleus. However, CPAP was first identified as a component of the centrosomal complex. The molecular interaction between CPAP and RelA evokes the possibility that RelA exists in centrosomes. Centrosomal location of factors related to transcription, such as p53 (38, 39) and BRCA1 (40, 41), has been reported and may be involved in centrosomal replication in a transcriptional activity-dependent or -independent manner. Further analysis of whether the interaction between CPAP and RelA affects centrosomal function may reveal new biological roles for RelA as well as CPAP.

Acknowledgments—We thank Dr. J. E. Visvader for providing pEFr-FLAG-CPAP, Dr. T. K. Tang for rabbit antiserum against CPAP, Dr. I. Thlianidis for pCMV-CBP, and Dr. A. Fukamizu for CBP deletion mutants. We thank M. Matsumoto-Kadowaki for help with confocal microscopy and Dr. T. Ohshima, T. Ego, Y. Miyanari, and others at our institute for helpful comments and discussions.

REFERENCES

1. Baldwin, A. S., Jr. (1996) *Annu. Rev. Immunol.* 14, 649–683
2. Ghosh, S., May, M. J., and Kopp, E. B. (1998) *Annu. Rev. Immunol.* 16, 225–260
3. Karin, M., Cao, Y., Greten, F. R., and Li, Z. W. (2002) *Nat. Rev. Cancer* 2, 301–310